processes

MDPI

Review

Modern Technologies of Hydrogen Production

Irina Stenina and Andrey Yaroslavtsev *

Kurnakov Institute of General and Inorganic Chemistry, Russian Academy of Sciences, Leninsky pr. 31, 119991 Moscow, Russia
* Correspondence: yaroslav@igic.ras.ru

Abstract: Transitioning to energy-saving and renewable energy sources is impossible without accelerated development of hydrogen energy and hydrogen technologies. This review summarizes the state-of-the-art and recent advances of various hydrogen production processes, including but not limited to thermochemical and electrolytic processes. Their opportunities and limitations, operating conditions, and catalysts are discussed. Nowadays, most hydrogen is still produced by steam reforming of methane, its partial oxidation, or coal gasification. Considerable attention is also paid to natural gas pyrolysis. However, hydrogen produced using these technologies has a lot of impurities and needs additional purification. A series of technologies for hydrogen purification, including its filtration through palladium alloy membranes, and membrane catalysis, allowing hydrogen production and purification in one stage, are discussed. The main way to produce carbon-free hydrogen is water electrolysis using low-cost energy from nuclear or renewable sources. Both conventional and novel methods of hydrogen storage and transportation, which are an important part of the hydrogen economy, are reviewed. Biohydrogen production technologies are also discussed. Finally, prospects for further work in this field are provided. This review will be useful to researchers and manufacturers working in this field.

Keywords: hydrogen production; hydrogen storage; steam reforming; water electrolysis; biomass; biohydrogen; membrane catalysis

check for updates

Citation: Stenina, I.; Yaroslavtsev, A. Modern Technologies of Hydrogen Production. *Processes* **2023**, *11*, 56. https://doi.org/10.3390/pr11010056

Academic Editor: Shu-Yii Wu

Received: 16 October 2022
Revised: 5 December 2022
Accepted: 22 December 2022
Published: 26 December 2022

1. Introduction

Economic and technological developments are impossible without energy consumption, which is constantly growing. At the same time, energy production leads to substantial environmental pollution. The main reasons for this are the emissions of carbon oxides, sulfur oxides, nitrogen oxides, and products of incomplete combustion of fossil fuels into the atmosphere. Particular attention is paid to carbon dioxide, which, according to a number of researchers, is the primary greenhouse gas. Therefore, the Paris Agreement focuses special attention on the energy sector. Significant efforts are being made to move towards energy conservation and new technologies associated with the use of environmentally friendly and renewable energy sources, such as solar panels, wind turbines, and tide stations [1,2]. However, to ensure an uninterrupted power supply, these sources should be used together with energy storage devices [3–8]. To level seasonal fluctuations in energy production, it is most appropriate to accumulate energy in the form of hydrogen.

Fuel cells can be used as autonomous or backup power sources [9–11]. To operate, they need hydrogen, which does not exist in a free state on the Earth. Moreover, hydrogen is currently required for a number of technologies, primarily for the production of ammonia, methanol, oil refining, metallurgy, and electronics. Hydrogen has long been considered as an alternative energy source due to its extremely high specific energy per unit mass—it is about three times higher than that of oil [12]. The total consumption of hydrogen in the world is about 115 million tons per year [13]. According to the International Energy Agency forecasts [14], hydrogen production should increase by 2.5 times in the next 30 years. Half of it will be spent on energy production, and another 30% will be spent for land transport,

while now only about 3% of hydrogen is spent for these purposes. However, according to [15], the production of hydrogen should grow faster and approach 700 million tons per year by 2050.

It is clear that hydrogen of different purities is required for different purposes. In metallurgy, in a number of chemical industries, or as a fuel, hydrogen can be used in a mixture with other gases [16,17], while high-purity hydrogen is required for microelectronics and the currently prevalent low-temperature fuel cells [11,18]. An important aspect is the impact of byproducts of hydrogen production on the environment, which largely determines the further development of various technologies for hydrogen production. Moreover, cost optimization for implementation should also be taken into account [19].

Nowadays, three quarters of hydrogen is produced by steam reforming of natural gas, and just under a quarter is by coal gasification [20]. According to other reports, oil refining also makes a significant contribution [21,22]. Nevertheless, it is obvious that technologies leading to pure hydrogen production based on electrolysis or photolysis of water are still less-demanded. A comparison of costs of hydrogen produced by different technologies and their energy efficiencies and carbon footprints is shown in Figure 1. Although coal gasification is the cheapest source of hydrogen, its high emissions (Figure 1) and level of hydrogen impurities make this approach less promising. Now, hydrogen production from coal is developing primarily in China [23]. Coal gasification can be performed directly under the ground. The product of this process is synthesis gas (syngas, a mixture of hydrogen and carbon monoxide), which contains methane, carbon dioxide, nitrogen, and small amounts of hydrogen sulfide [24,25].

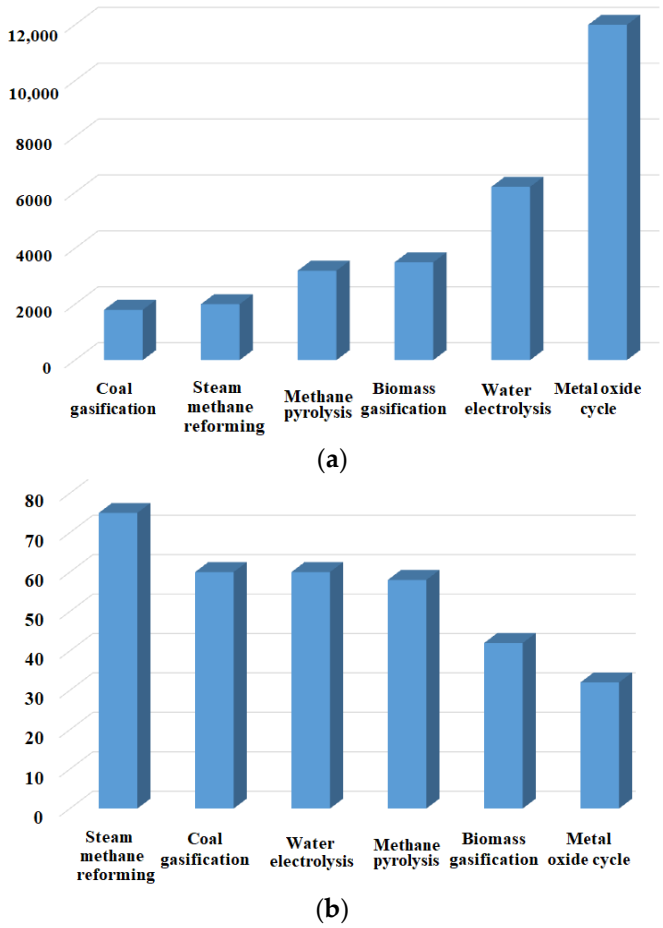

Figure 1. *Cont.*

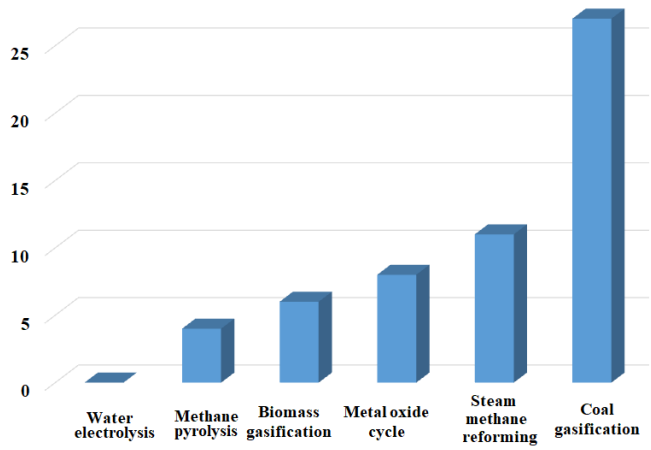

(**c**)

Figure 1. (**a**) Costs of hydrogen (EUR/t) produced by different technologies; (**b**) their energy efficiencies (%); and (**c**) carbon footprints (t_{CO2}/t_{H2}) [26–32].

In this review, the main methods of hydrogen production and the prospects for their development are discussed.

2. Steam Methane Reforming

The most attractive and common approach for hydrogen production is steam reforming of methane (SRM) (Figure 2) [33], which can be described by the following reaction:

$$CH_4 + H_2O \leftrightarrow CO + 3H_2,\ \Delta H^0 = 206\ kJ/moL \quad (1)$$

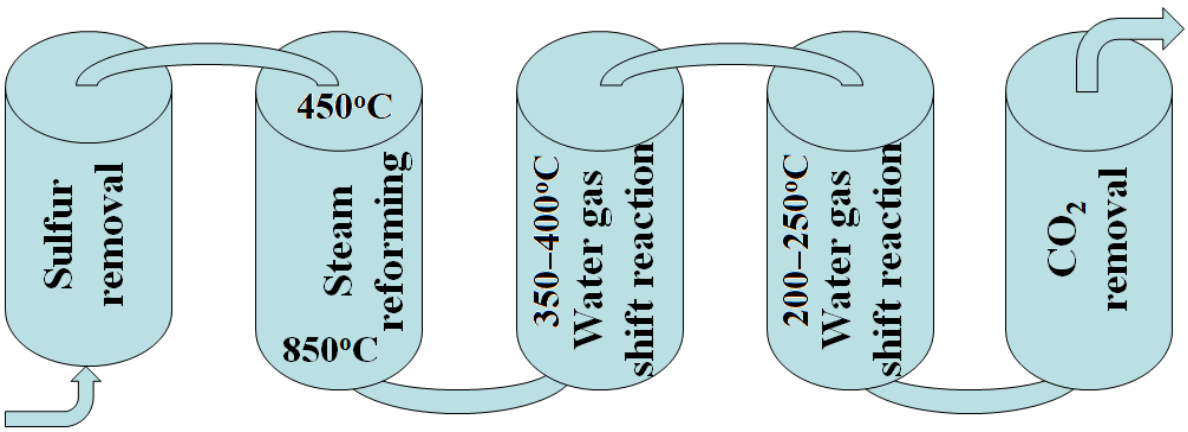

Figure 2. Scheme of steam–methane reforming for H_2 production.

This approach enables reaching a maximum yield of hydrogen (up to 3 moles of hydrogen and 1 mole of CO per 1 mole of methane). Moreover, carbon monoxide can interact with water steam at temperatures of 200–400 °C to form carbon dioxide and generate additional hydrogen (water–gas shift reaction) (Figure 2):

$$CO + H_2O \leftrightarrow CO_2 + H_2,\ \Delta H^0 = -41\ kJ/moL \quad (2)$$

However, since the main process (Equation (1)) is endothermic, it requires high temperatures, at which the CO_2 yield is limited [34]. The need for high temperatures is also determined by the fact that activation of a highly symmetrical molecule of methane with strong C–H bonds requires a lot of energy. Moreover, as temperature decreases, the carbon

deposition on catalyst proceeds more intensively. It is also noted that the conversion of methane increases with increasing the steam-to-methane ratio up to five [35]. Both of the above processes (Equations (1) and (2)) are catalytic and can be accelerated by both noble and transition metals. In the series of noble metals, the catalytic activity decreases in the series Ru > Rh > Ir > Pt [36,37]. High reforming activities and low rates of carbon formation are among advantages of these catalysts [38–40], but due to high cost, their use is limited. In this regard, the attention of researchers was attracted to the iron family metals [41]. However, iron is prone to oxidation, while cobalt is relatively expensive and toxic; therefore, catalysts based on nickel, whose activity is comparable to that of platinum and iridium, are more in demand [42,43]. The use of bimetallic catalysts is also effective and increases their activity, selectivity, and durability in comparison with monometallic catalysts, as well as limits carbon formation, oxidation, and sintering [44–48]. It is worth noting the use of catalysis to lower the reaction temperature [49].

The most serious problems are sulfur poisoning and activity loss due to rapid sintering and carbon formation (Figure 3). The use of supports, predominantly oxides, such as alumina and silica, increases the conversion degree and reduces the poisoning effect [50–52]. Even more effective are spinels ($MgAl_2O_4$, $ZnAl_2O_4$), which reduce carbon deposition and increase resistance to sintering [53,54], doped zirconia and ceria, etc. [55–57]. Their advantages include improved conversion and decreased carbon deposition [35,56]. The activation energy and reaction rate are significantly affected by the support's nature, dispersity, and structure [34,54,58–61].

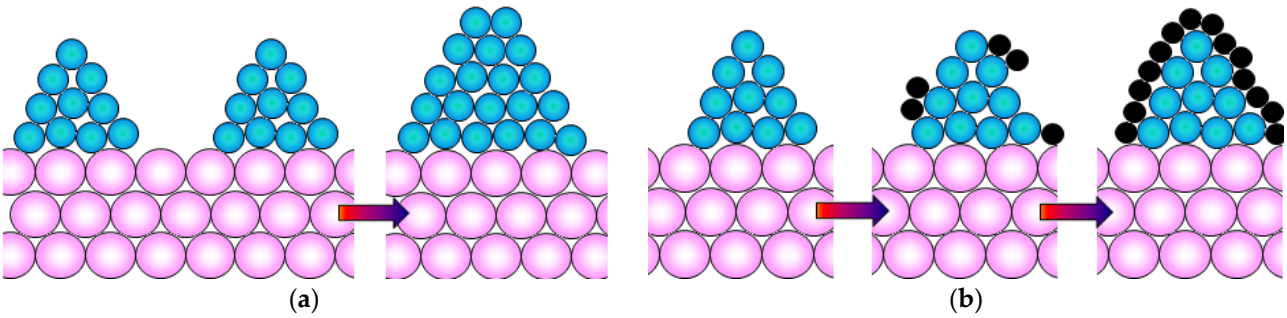

Figure 3. Schematic illustrations of the sintering (**a**) and coking (**b**) processes for SRM catalyst. Pink, blue and black balls denote support, metal catalyst and carbon, respectively.

A promising approach is the selective extraction of one of the products (hydrogen or carbon dioxide), leading to a shift in the thermodynamic equilibrium and thus increasing the hydrogen yield. Extraction of hydrogen is usually performed via a process of membrane catalysis, which we write about below. CO_2 extraction is also very promising [62–64]. Amines [37,65], calcium compounds [66,67], alkali metal zirconates, and silicates [68–71] have been used to absorb carbon dioxide. Direct extraction of CO_2 is possible using anion exchange membranes [72]. Using this approach, the hydrogen yield can be significantly increased [71,73]. Thus, according to [74], it can be more than 90%.

3. Partial Oxidation of Methane

Partial oxidation of methane (POM) is another common approach to hydrogen production [75–78]. In contrast to steam methane reforming, this process produces less hydrogen (Equation (3)) and is more difficult to control, since the released hydrogen is easily oxidized by oxygen. However, its undoubted advantage is that it is exothermic, although the released heat is small.

$$CH_4 + 1/2O_2 \leftrightarrow CO + 2H_2,\ \Delta H^0 = -8.6\ \mathrm{kJ/moL} \quad (3)$$

The product of Reaction (3), proceeding at 600–950 °C, is a POM syngas [79–82], which is often used for the synthesis of chemicals (methanol, dimethyl ether, etc.). High temperatures and low selectivity of the process (Equation (3)) lead to the formation of carbon as a byproduct, which deactivates catalysts [83–85]. At the same time, it is possible to further oxidize CO by steam (Equation (2)) by cooling the product flow to increase the hydrogen yield [86–88]. To compensate for the heat released, partial oxidation can be combined with steam reforming of methane. This is the so-called autothermal reforming of methane (Figure 4) [89].

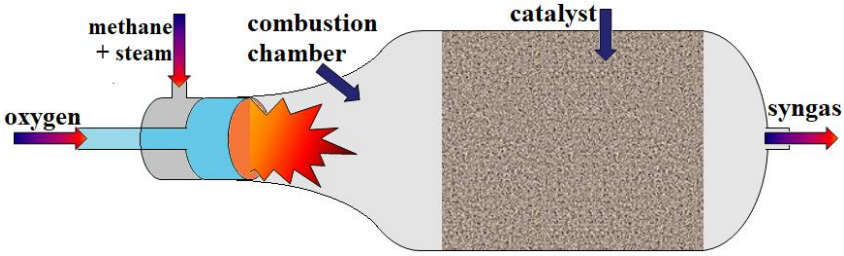

Figure 4. Scheme of the reactor for autothermal reforming.

Since partial oxidation of methane requires activation of the same bonds as for its steam reforming and many other processes, which are described in more detail below, the catalysts used for both processes turn out to be very similar. First of all, we are talking about platinum-group metals [83–85,90–93], among which rhodium should be noted [77,94,95]. Rhodium alloys with various transition metals are used to improve methane conversion and productivity [76,96–99]. At the same time, considerable attention is paid to transition metals, predominantly nickel [100]. The use of lanthanum–nickel alloys leads to an increase in the CO_2 fraction in the reaction products [90].

One of the main problems of nickel and some other catalysts are oxide and carbon deposits. To suppress their formation, supports based on oxides of zirconium, titanium, cerium, and lanthanum are used [95,101–103]. Support optimization is also used to increase the degree of methane conversion and the CO_2 fraction in the POM products [104].

To date, an approach is also being developed where the oxygen sources (oxygen carriers) for the partial oxidation of methane are oxides of nickel, copper, iron, and other metals, which are reduced to a metal and then oxidized again (Figure 5) [63,105,106]. As a development of this approach, it is possible to combine oxidation with the capture of released CO_2 by calcium oxide [107]. However, according to [31], the cost of hydrogen produced using this approach exceeds the cost of hydrogen produced using any others.

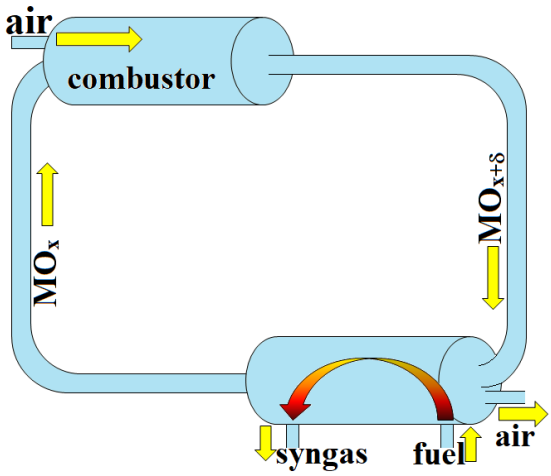

Figure 5. Scheme of hydrogen production with the use of chemical looping combustion.

4. Carbon Dioxide Reforming

Another common approach is the carbon dioxide reforming of methane, which is often called 'dry reforming of methane (DRM)', since CO_2 is a substitute for water in steam methane reforming [108,109]:

$$CH_4 + CO_2 \leftrightarrow 2CO + 2H_2, \Delta H^0 = 248 \text{ kJ/moL} \quad (4)$$

This process is endothermic, and its heat is comparable to that of steam reforming of methane. Accordingly, this process proceeds at high temperatures (700–1000 °C). A CO-rich synthesis gas is produced using this technology, and therefore, DRM can hardly be considered as a method for hydrogen production. Even in the case of DRM syngas use for the synthesis of organic compounds, it is better to combine this process with steam methane reforming (Equation (1)) to increase the H_2/CO_2 ratio up to two [110,111]. Interest in dry reforming of methane is primarily stimulated by the problem of CO_2 management [65,112].

A lot of attention is drawn to the choice of catalysts. The DRM process proceeds via sorption of methane and carbon dioxide molecules, which lowers their dissociation energy [113]. Wei et al. showed that catalysts with optimum binding of oxygen and carbon atoms to the catalyst surface exhibit maximum catalytic activity [114]. As a rule, despite high binding energy, the activation of CO_2 molecules turns out to be lower. Bitter et al. suggested that methane is activated on metal sites, while CO_2 is activated on acid sites of the support [115].

Platinum-group metals, primarily ruthenium and platinum, exhibit high catalytic activity in the dry reforming of methane (Table 1), which allows the process to proceed at relatively low temperatures [115]. However, nickel catalysts are more often used for this process due to their lower cost [110,112,116,117]. Moreover, the activity of catalysts in DRM depends on catalyst support (primarily its basicity and redox ability) and metal–support interactions (Table 1). The basicity of the support determines its activity in sorption and activation of gas molecules, while redox properties can promote the catalytic process as a whole and determine the main directions of the process and its byproducts. Thus, supports are primarily used to ensure high activity of a catalyst material and to minimize carbon deposits [118–120].

Table 1. Comparison of the catalyst activity in DRM (feed-gas ratio CH_4:CO_2 = 1:1).

Catalyst		T (°C)	Conversion (%)		Time on Stream (min)	Reference
Metal	Support		CH_4	CO_2		
Ni	La_2O_3	650	62	67	3000	[121]
Ni	SiO_2/TiO_2	650	65	54	1440	[122]
Ni	Activated carbon	900	80	98	500	[123]
Ni	$MgO/Ce_{0.8}Zr_{0.2}O_2$	800	95	96	12,000	[124]
Ni	Al_2O_3	800	63	82	1200	[125]
Ni	CeO_2–Al_2O_3	850	100	100	600	[126]
Ni	SBA-15	800	88	89	300	[127]
Ni-Co	SBA-15	25	29	19	600	[128]
Ni-La	SBA-15	750	88	96	660	[129]
Co	Sr/La_2O_3	800	94	99	1800	[130]

5. Methane Pyrolysis

Unfortunately, all the processes described above lead to the production of carbon oxides as byproducts and, with the exception of CO_2 reforming, do not solve the carbon footprint problem [131]. In this regard, in recent years, interest in the well-known process of natural gas pyrolysis (Equation (5)) has increased significantly.

$$CH_4 \leftrightarrow C + 2H_2, \Delta H^0 = 74.8 \text{ kJ/moL} \quad (5)$$

Based on the stoichiometry of reaction (5), solid carbon is the only byproduct, and there are no greenhouse emissions, which contribute to atmospheric pollution with carbon oxides [131–134]. Therefore, it is often believed that it is possible to produce hydrogen with zero carbon footprint, which should help solve the carbon management problem [131,135–137]. The carbon byproduct generated by methane pyrolysis is predominantly a carbon black that can be used in metallurgical (steel) industry as carbon additive or production of carbon fibers for variety applications, including car tires. There is an opinion about the possibility of using carbon in direct-carbon fuel cells [138]. However, assuming that pyrolysis will provide a significant portion of hydrogen production, the amount of carbon will significantly exceed the needs for its use.

Unlike previous technologies, in methane pyrolysis there are no reagents with a chemical affinity for its components, and therefore maximum activation energy is required. In this regard, its implementation is possible only at temperatures above 1100 °C. The reaction proceeds through the formation of methyl radicals and hydrogen atoms and further similar transformations of sequentially formed hydrocarbons. The temperature of pyrolysis can be reduced by using catalysts that promote these processes initiated by molecular [139,140] or dissociative adsorption of hydrocarbons [141–143]. Dissociation of hydrocarbons is facilitated by the transfer of electrons from the C–H bonds of methane to vacant d-orbitals of transition metals [144–148]. An increase in catalytic activity in the series Fe < Co < Ni has been reported [144,146,149]. Nickel catalysts exhibit maximum activity (Table 2), which rapidly decreases due to blockage by the formed carbon layer [146,148,150].

Iron-based catalysts exhibit significantly lower activity in methane pyrolysis (Table 2), but at the same time, they are cheaper and show better resistance towards carbon deposits. Fe catalysts can operate stably at temperatures up to 1000 °C [145,151–153] due to higher carbon diffusion, which is three orders of magnitude higher than that of nickel-based catalysts [131,145]. This helps to 'clean' the catalyst surface and maintain its activity for a longer time. The least-demanded are cobalt catalysts because of their toxicity and lower activity compared to nickel [154,155].

Considerable attention is also paid to oxide supports, which are designed to prevent both the agglomeration and the deactivation of catalyst particles [150,153,156,157]. In catalytic pyrolysis, nickel-based alloys with cobalt, palladium, copper, and some other metals are also actively used. The second metal is used as a so-called promoter, leading to additional acceleration of the process [145,146,158]. It should be noted that the role of the second metal in this case is not quite traditional. Often, it is introduced to increase the rate of carbon diffusion in the alloy, enabling it to work at higher temperatures and providing less deactivation of nickel by carbon deposits [159–161].

Table 2. Comparison of the catalyst activity in methane pyrolysis.

Catalyst	T (°C)	Feed Gas Composition	Conversion of CH_4 (%)	Reference
Ni/SiO_2	650	CH_4	85	[162]
55% Ni − 15% $Cu/MgO{\cdot}Al_2O_3$	675	CH_4	80	[163]
12.5% Ni − 12.4% Co/La_2O_3	700	N_2:CH_4 = 1:9	82	[164]
50% Ni − 10% Fe/Al_2O_3	675	N_2:CH_4 = 7:3	68	[144]
50% Ni − 10% Pd/Al_2O_3	675	N_2:CH_4 = 7:3	75	[165]
20% $Fe/WO_3 + ZrO_2$	800	N_2:CH_4 = 1:2	90	[166]
Fe − 5.1% Mo/Al_2O_3	750	CH_4	69	[167]
65% Fe/Al_2O_3	750	CH_4	70	[168]
Fe sponge	1000	CH_4	85	[169]

Even less-active are carbon catalysts (activated carbon, carbon black, acetylene black, etc.), which operate only at temperatures from 800 to 1000 °C [131,170–172]. At the same time, they are widely used in this process due to their low cost and high stability, since in this case the process becomes autocatalytic and only a small amount of catalyst is needed to initiate it. Moreover, carbon catalysts are also stable to sulfur and other impurities contained in natural gas [131,173]. Active catalytic centers of carbon catalysts are believed to have multiple defects on their surface, which is confirmed by the dependence between the number of defects in graphene layers, initial temperatures, and reaction rates [174].

Recently, considerable attention has been paid to methane pyrolysis over molten metals or salts. This results in the long-term activity of catalysts due to prevention of rapid carbon deposition [133,175–180]. An additional advantage is the high heat capacity of the melt, which ensures the stability of the catalytic process.

Despite the great attention to hydrogen production by methane pyrolysis and optimism regarding its environmental friendliness, this method has many disadvantages. Among them, first of all, it is worth mentioning the high energy consumption. Moreover, formation of carbon as a co-product is a huge problem, as through this process we lose half of the potential methane energy. Moreover, as was mentioned above, the amount of carbon formed in the production of potentially demanded hydrogen is an order of magnitude higher than the need for carbon [131–133]. Since methane pyrolysis proceeds at high temperatures and is not quite selective, the hydrogen produced still contains a lot of impurities and also requires deep purification.

6. Reforming of Biomass and Bio-Alcohols

Biomass is an excellent renewable feedstock and can cover a major part of humanity's needs for precursors for organic synthesis and energy carriers. There are various approaches to its processing. For example, biomass can be used as a source of methane (biomethane) and, using approaches similar to those described above, be converted into hydrogen-rich synthesis gas [181–183]. Steam reforming of lignin [184,185], products of fermentation of biomass containing an aqueous solution of ethanol [186–189] or methanol produced by dry distillation of lignin seems to be even more attractive. Many authors note the attractiveness of the direction associated with the reforming of aqueous solutions of various organic compounds, including biomass processing products, wastewater, etc. in milder conditions (230–270 °C and autogenous pressure)—so-called 'aqueous phase reforming' [184,190,191]. It should be noted that at present, biomass is also considered a promising and renewable carbon source for the production of chemicals.

The advantage of alcohol steam reforming is milder reaction conditions, e.g., lower temperatures, compared to SMR. For ethanol and methanol, the overall reactions of alcohol steam reforming can expressed by Equations (5) and (6), respectively:

$$C_2H_5OH + 3H_2O = 2CO_2 + 6H_2,\ \Delta H^0 = 157\ kJ/moL \quad (6)$$

$$CH_3OH + H_2O = CO_2 + 3H_2,\ \Delta H^0 = 50\ kJ/moL \quad (7)$$

Although the main products of these processes are hydrogen and CO_2, other byproducts, e.g., CO, which negatively affect the operation of low-temperature fuel cells, are also presented. However, their concentrations are lower than in SRM, while the hydrogen yield is higher. Therdthianwong et al. reported the implementation of this process without any catalyst at a pressure of 25 MPa in supercritical water in the temperature range of 500–600 °C [192]. In the catalyst's presence, these processes proceed even more easily. Thus, the steam reforming of ethanol usually proceeds at temperatures of 400–500 °C, while in the case of methanol, the reaction temperature is in the range of 300–400 °C [193].

Despite a significant difference in temperatures with methane and ethanol steam reforming, the same catalysts (noble metals, copper, or nickel) are often used for these processes [194–197]. The reason for this is that its initiation also requires activation of C-H and O-H bonds [198]. The activity of catalysts based on noble metals is usually higher, but

copper and nickel are used more often due to their low costs. As in the processes described above, alloys of these metals are often used to increase the catalytic activity [198–200].

Perhaps in steam reforming of alcohols even more attention is paid to choosing catalyst supports [201,202]. In accordance with the predominant opinion, the role of metal in this process is the activation of alcohols, while sorption of water vapor occurs on the support (Figure 6). In this case, the main catalytic transformation processes described by Reactions (6) and (7) occur at the interface between the catalyst and its support [187]. Finely dispersed oxides of metals with a charge of 2–4 (zinc, aluminum, silicon, etc.) are commonly used as a support [203–209]. Obviously, the support surface area should be considered. For example, it was shown that the activity of zirconia-supported catalysts increases by increasing the dispersion of ZrO_2 particles [210]. In this regard, mesoporous oxides are also used as supports [195,211]. The catalyst activity can be additionally increased by doping supports based on zirconia or titania with trivalent elements or cerium ($M_XZr\ (Ti)_{1-X}O_{2-\delta}$) [212,213], which increase the mobility of oxygen ions in these oxides [214].

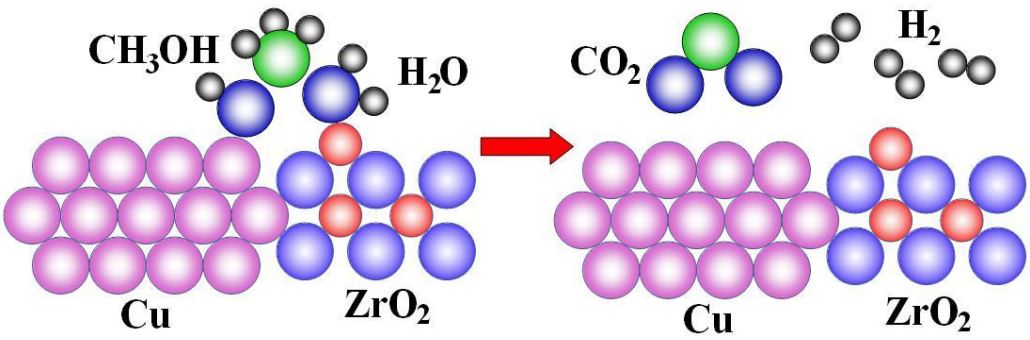

Figure 6. Scheme of methanol steam reforming with the use of Cu/ZrO_2 catalyst.

The use of highly dispersed carbon supports, including carbon blacks and nanodiamonds, in steam reforming of alcohols has been reported [215]. At first glance, their activity seems not quite clear, since carbon is not an active water sorbent. It has been shown that its activity is determined by the high content of oxygen-containing groups (OH, CO, and COOH) on the carbon particle surface and that it increases upon special surface treatment [193,216]. A successful combination of catalyst and support reduces the CO concentration in the reaction products.

In recent years, biological methods of hydrogen production from biomass have been actively developed. They are based on the ability of microorganisms (primarily bacteria) to consume biomass and release hydrogen (the so-called microbial conversion of biomass). Dark (as no light is required) fermentation is the simplest approach, which uses anaerobic bacteria to produce enzymes (it is a part of their anaerobic digestion) capable of converting biomass into hydrogen, organic acids (mostly acetic and byteric acids), and carbon dioxide [217–219]. However, the hydrogen yield is significantly limited by the metabolism of the bacteria (once the hydrogen partial pressure exceeds a critical value, a different metabolic pathway can be switched on) and depends on many factors such as substrate, temperature, pH, toxic substances, competitive bacteria, etc. At the same time, there is information on increased hydrogen yield obtained, for example, by the addition of metal ions and oxide nanoparticles [218] or the use of genetically modified bacteria [220]. A significant advantage of this method is the ability to produce hydrogen around-the-clock. Increased hydrogen yield is provided by photofermentation under anaerobic conditions, which allows processing of biomass into hydrogen using light energy for photosynthesis [219,221].

The problem with all the methods of microbial biomass conversion (including the microbial electrolysis described in the last section) is the low hydrogen yield, and therefore, these promising methods are still at an early stage of development. Another problem

with many of them is the incomplete conversion of biomass and the formation of waste containing a large amount of fatty acids that need further processing [222]. However, according to [223], by 2050, biomass will provide more than 25% of energy demand. The reason for this is that the absorption of CO_2 during the formation of biomass compensates for its emissions during energy production, which leads to a carbon neutral scenario [224].

7. Reversible Hydrogen Carriers

One of the serious problems of hydrogen energy is storage and transportation of hydrogen, as it is difficult to liquefy it. In the case of compressed hydrogen, the high weight of gas cylinders/tanks is the main limitation to its transportation (tank weight is more than an order of magnitude higher than that of hydrogen). Transportation of liquid hydrogen is no less problematic [11,225]. In this regard, chemical methods of hydrogen storage have become very popular in recent years (Figure 7). The highest weight-storage density of hydrogen is achieved in metal borohydrides (Figure 8) [226]. However, there are significant problems with their hydrolysis products, which are boric acid or its salts. They are toxic and not easily rehydrogenated to borohydrides. In this regard, the ammonia cycle (Equation (8)) has significant advantages.

$$2NH_3 \leftrightarrow N_2 + 3H_2,\ \Delta H^0 = 92\ kJ/moL \quad (8)$$

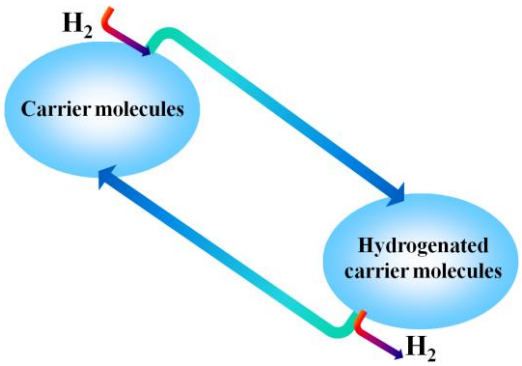

Figure 7. Hydrogen carrier reaction pathways.

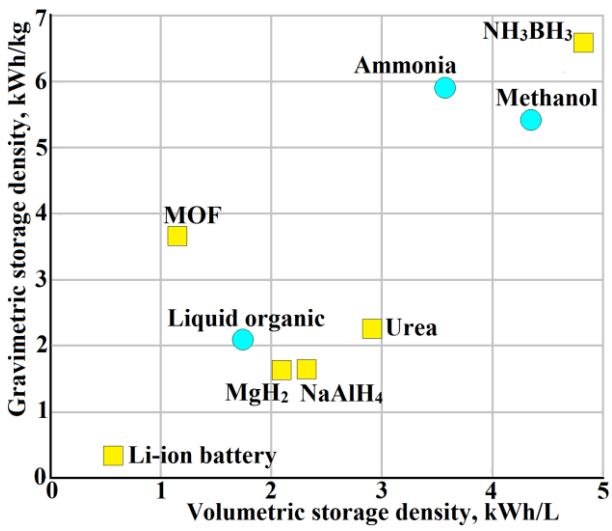

Figure 8. Gravimetric and volumetric energy storage densities for some solid (yellow squares) and liquid (blue circles) carriers.

One of the ammonia decomposition products is nitrogen (Equation (8)), which can be discharged into the atmosphere and is relatively easily recovered from it through liquefaction and distillation. This method is second only to the borohydride method in terms of gravimetric hydrogen density [227]. Ammonia production is the well-known Haber–Bosch process. Both for it and for the reverse process (dehydrogenation of ammonia), an important task is the selection of a catalyst, primarily for the efficient adsorption of nitrogen and hydrogen. For this purpose, catalysts based on iron and ruthenium are most often used [228]. Mayenite ($Ca_{24}Al_{28}O_{64}$), with cavities capable of efficiently absorbing hydrogen, should be mentioned among oxide systems [229,230]. The ammonia cycle is being actively developed in a number of countries, but its use is associated with a number of problems that should be mentioned, among which are the toxicity of concentrated ammonia and incomplete conversion limited by the thermodynamic equilibrium. The ability of ammonia to cause fuel cell degradation even at a low content in the fuel (on the order of ppm) should be also noted [231]. Some disadvantages can be effectively mitigated by using membrane catalysis [33,232].

Liquid organic hydrogen carriers provide the most comfortable transportation by transport or in pipelines. Cyclic compounds, which transform into aromatic compounds upon dehydrogenation (benzene, toluene, cyclohexane, methylcyclohexane, decalin, etc.), predominate among them [233–235]. Typical examples are the benzene cycle based on hydrogenation of benzene and dehydrogenation of cyclohexane:

$$C_6H_{12} \leftrightarrow C_6H_6 + 3H_2,\ \Delta H^0 = 206\ \mathrm{kJ/moL} \quad (9)$$

One of the most common cycles is the toluene cycle due to its high selectivity, reversibility, and the absence of carcinogenic products [236]. The hydrogen storage capacity of toluene is 6.1%, while the maximum theoretical storage capacity of liquid organic carriers reaches values just above 8%.

Heterocyclic compounds are considered promising hydrogen carriers due to their reduced dehydrogenation temperature. Among them, the most widely represented systems include nitrogen–heterocyclic compounds [237–243]. There are also works on cyclic hydrocarbons with sulfur atoms [244] and boron [245].

Most often, catalysts based on platinum-group metals on oxide supports are used for hydrogenation and dehydrogenation of organic carriers. Their high catalytic activity allows, in some cases, achieving full dehydrogenation at temperatures of about 300 °C [233,243,245–254]. In recent years, much attention has been paid to cheaper catalysts that do not contain platinum-group metals, e.g., iron and manganese-based catalysts [255–257].

The advantages and disadvantages of various storage methods are summarized in Table 3.

Table 3. Comparison of various hydrogen storage methods.

Storage Method	Advantages	Disadvantages
Compressed H_2	- Commercialized	- Low volumetric storage capacity - High pressure - Limited storage time - Special transportation configuration - Safety issues

Table 3. *Cont.*

Storage Method	Advantages	Disadvantages
Liquid H_2	- Increased storage capacity (1.6–1.7 times more than that of compressed H_2) - Commercialized	- High liquefaction energy (requires cryogenic temperature (−253 °C)) - Boil-off effect - Hydrogen leakage - Special transportation configuration - Safety issues
Cryo-compressed H_2	- Increased storage capacity (2–3 times more than that of compressed H_2)	- High energies of compression and liquefaction - Low availability of infrastructure - High cost of infrastructure
Solid carrier	- Lightweight; high storage density; superior reversibility and cycle stability; high charging–discharging rate (forms materials with physisorption) - Reversibility; high volumetric density (for materials with chemisorption) - Unlimited storage time	- Requires low temperatures or high pressures to store and elevated–to release H_2 (for materials with physisorption) - Poor sorption kinetics; irreversible reactions (materials with chemisorption) - Requires a new infrastructure (immature technology)
Ammonia	- High hydrogen storage capacity - High auto-ignition temperature (650 °C)	- Toxicity/safety issues - High energy input
Liquid organic hydrogen carrier	- Excellent safety - High gravimetric and volumetric hydrogen storage capacity - Unlimited storage time	- Requires elevated temperatures for both hydrogenation and dehydrogenation - Limited experience

8. Hydrogen Purification and Membrane Catalysis

Nowadays, the most common type of devices for power generation using electrochemical oxidation of hydrogen or hydrogen-containing fuel are proton-exchange membrane fuel cells operating at temperatures up to 100 °C [11]. High-purity hydrogen is required for them. They should not contain even trace CO impurities, which irreversibly poison platinum catalysts at these temperatures [258–260]. Unfortunately, hydrogen produced using all the processes described above is not suitable for direct use in such devices and must be deeply purified. Hydrogen can be purified using polymeric, molecular sieving carbon, and other membranes with nanosized pores [261–263]. However, all of them can only reduce the impurity content. This can also be achieved using membranes with mixed oxygen and electron conductivity [264]. Membranes are also often used in membrane reactors for the safe conversion of natural gas in the presence of oxidizers [34,265,266].

Extremely high-purity hydrogen can only be obtained using dense metallic membranes based on palladium and its alloys, through which only hydrogen can permeate [267]. It should be noted that vanadium is more permeable to hydrogen, but V-based membranes are prone to extreme hydrogen embrittlement. Alloys of palladium with copper, silver [268–272], or ruthenium [273,274] are characterized by the highest hydrogen permeability. The widespread use of palladium membranes is limited by their high cost and relatively low productivity, which can be increased by reducing the Pd-membrane thickness. However, the possibility of this approach is limited by the need to maintain sufficient membrane strength to withstand a significant pressure drop. Another approach is the creation of composite membranes, e.g., films based on highly porous oxide supports, in particular, anodic alumina, coated with palladium alloys [275,276]. Oxide supports provide mechanical strength, while the high selectivity of hydrogen extraction is determined by the Pd-coating, the small thickness of which, along with the porosity of the oxide layer, pro-

vides high hydrogen permeability. Vanadium-based membranes with palladium coating combine both high hydrogen permeability and resistance to embrittlement [277].

Membrane reactors are also used to produce high-purity hydrogen from methane, alcohols, and other reagents in one stage using membrane catalysis (Figure 9) [33,278–280]. Among other advantages of this approach, it is worth noting the possibility of reducing the process temperature and increasing the hydrogen yield by removing it from the reaction zone and thereby shifting the thermodynamic equilibrium [198,216,281–283].

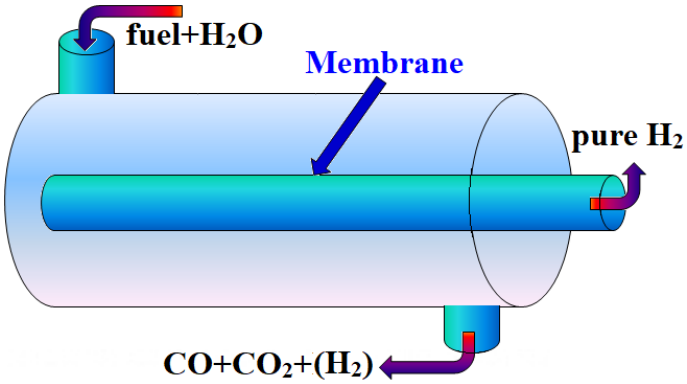

Figure 9. Scheme of hydrogen production with the use of membrane catalysis.

The most obvious example is the water–gas shift reaction described by Equation (2). The removal of hydrogen from the reaction zone leads to an increase in the CO conversion and increases the hydrogen purity [284,285]. A recent publication [116] describes various approaches to hydrogen production using ceramic membranes. However, membranes based on palladium alloys, which produce high-purity hydrogen, are more commonly used in these processes [33]. It should be noted that the water-gas shift reaction is most suitable for increasing both the hydrogen yield and its purity in the SRM and POM processes. However, these processes proceed at high temperatures, which are unfavorable for the water–gas shift reaction. In this regard, it is preferable to divide the process into two or three stages: in the first stage, methane conversion occurs at high temperatures, and then the water–gas shift reaction occurs through the reaction of CO and excess water vapor at temperatures of 200–450 °C (Figure 2) [286,287]. For example, Tokyo Gas Company produces high-purity hydrogen from methane with the additional oxidation of CO at temperatures of 400–500 °C [288].

Alcohols can be obtained from biomass and can be considered a renewable feedstock. The steam reforming of alcohols proceeds at lower temperatures, which are actually optimal for both the main process (reforming) and the water–gas shift reaction. Therefore, in this case, the process is carried out in one stage, significantly increasing the conversion of alcohols above the thermodynamic equilibrium [289]. Thus, the application of membrane reactors with membranes made of palladium–silver or palladium–ruthenium alloys with Cu- or Ru-based catalysts at temperatures of 200–350 °C achieves methanol conversion of 85–100% with high-purity hydrogen yield of 40–97% [198,290]. Similar results have been obtained for composite membranes based on anodic alumina with a selective palladium layer [281].

In the case of ethanol steam reforming in membrane reactors, the ethanol conversion varied from 40 to 99–100%, while the high-purity hydrogen yield can be low and varied from 10 to 93% [291]. The main reason for this is a higher process temperature (400–600 °C), which determines the lower selectivity of the process and worsens the thermodynamics of the water–gas shift reaction. Membranes made of both palladium–copper or palladium–silver alloys [291–294] and a wide range of composite membranes have been used [291,295–298]. Catalysts based on noble metals (Pt, Ru, or Ir) as well as catalysts based on nickel, cobalt, and copper have been used.

Acetic acid is one more product of biomass fermentation. It can also be converted into hydrogen according to Equation (10):

$$CH_3COOH + 2H_2O \leftrightarrow 2CO_2 + 4H_2,\ \Delta H^0 = 134.9\ kJ/moL \quad (10)$$

In Reaction (10), the maximum yield of pure hydrogen in the permeate zone reached 70% using reactors with palladium–silver membranes and Ni catalysts at a temperature of 400–450 °C [299].

9. Water Electrolysis

Electrolysis of water using renewable energy sources is the main completely environmentally friendly method of hydrogen production today. However, its disadvantages are obvious [300]. The maximum efficiency of electrolyzers and fuel cells under the most favorable conditions (at low currents) is about 70%. Therefore, at best, only half of the energy spent to produce such hydrogen can be generated back from it. Moreover, electrolyzers are quite expensive. In this regard, at present, hydrogen produced by electrolysis is usually 2–4 times more expensive than hydrogen produced from natural gas [301,302].

The thermodynamic potential of the water electrolysis reaction is 1.23 V. However, electrolysis is actually carried out at even higher potentials. To understand the reason for this phenomenon, consider the electrolysis mechanism. According to the current concept, the hydrogen evolution reaction (HER) proceeds by the following pathways (Equations (11)–(13)):

$$H^+ + e^- = H_{ad}, \quad (11)$$

$$H^+ + e^- + H_{ad} = H_2, \quad (12)$$

$$2H_{ad} = H_2, \quad (13)$$

where H_{ad} represents an adsorbed hydrogen atom on the catalyst surface. It can act as a reaction center for the reduction of another H^+ ion (Equation (12)) or can react with the second adsorbed hydrogen atom to form a hydrogen molecule (Equation (13)) [303]. In alkaline electrolyzers with anion-exchange membranes, processes (11) and (12) proceed by the following equations [304]:

$$H_2O + e^- = OH^- + H_{ad}, \quad (14)$$

$$H_2O + e^- + H_{ad} = OH^- + O_2. \quad (15)$$

In any case, an adsorbed (unbonded) hydrogen atom is formed in the first step. Obviously, a much higher potential than 1.23 V is generally needed for the H–O bond to break in the acid medium. The same problems are typical for the oxygen evolution reaction (OER). Thus, both these processes require additional energy, which is expressed in terms of overvoltage in electrochemistry (analogous to the activation energy in kinetics). It is the high overvoltage of HER and OER reactions that is one of the main problems that limit the water electrolysis application [305]. This overvoltage can be reduced by adsorption of radicals formed at the first stages of electrolysis to reduce energy losses during their formation. However, as the sorption energy increases, the desorption of products from the surface becomes more difficult. Therefore, the dependence of the current density on the metal–H binding energy has a volcano-like pattern (Figure 10), as for many other processes of hydrogen production, and platinum-group metals (Pt, Rh, and Ir) with mild hydrogen adsorbtion energies are the most favorable for the electroreduction of hydrogen [306,307]. An additional contribution to the overvoltage is made by the concentration effects and the resistance of electrodes and the electrolyte [308]. Moreover, the contribution of ohmic losses is higher with increasing electrolysis intensity, since

$$U_{Ohm} = IR, \quad (16)$$

where R is the total resistance of the electrolysis cell, and I is the current.

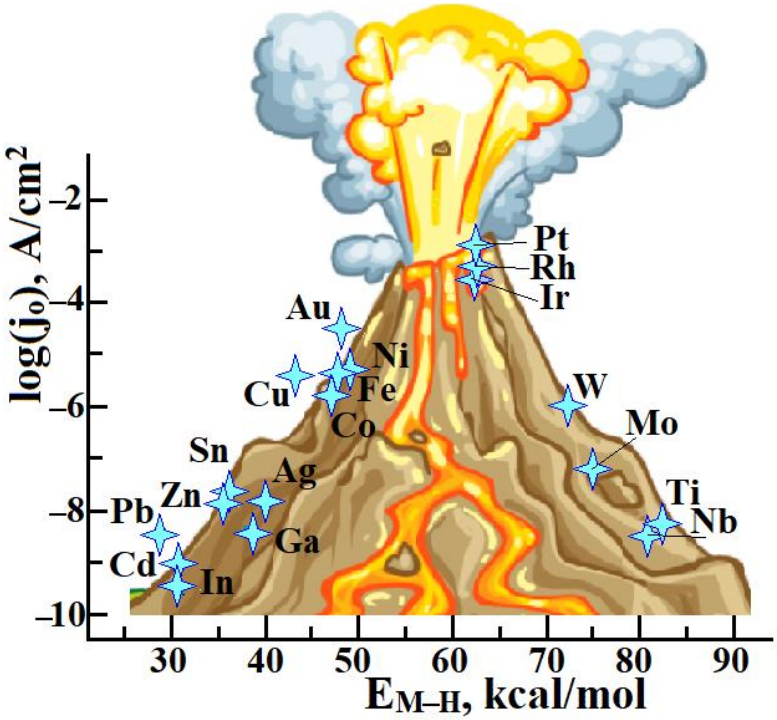

Figure 10. Dependence of exchange current density vs. the M–H bond energy in acidic media (according to [306]).

There are four main electrolysis methods, depending on the type of membrane used: (1) proton-exchange membrane water electrolysis, (2) alkaline electrolysis, (3) high-temperature electrolysis with solid oxide membranes, and (4) microbial electrolysis (Figure 11, Table 4). Proton-exchange membrane electrolyzers use Nafion-type perfluorinated membranes and noble metal-based electrocatalysts that are stable during the operation of such cells [309–311]. The latter are the most widespread due to their compactness, fast response, and high efficiency. Their disadvantage is the high cost of materials and a whole cell. Base-metal electrocatalysts and non-perfluorinated membranes can be used in alkaline electrolysis, which reduces the cost [312]. Initially, cheap porous membranes from asbestos impregnated with an alkali solution were used in alkaline electrolysis cells [313]. In recent years, a new approach associated with the use of polymeric anion-exchange membranes has been actively developed. However, the hydrogen electroreduction rate in alkaline media is usually 2–3 orders of magnitude lower than that in acidic media [313,314]. High-temperature solid oxide electrolysis requires a lot of energy due to high operating temperatures and pressures [315]. At the same time, a number of researchers note that the use of steam at elevated temperatures increases the electrolysis efficiency [316,317]. Electrolysis using renewable energy sources is the most promising. However, the stochasticity of these sources results in the variability of their operation and requires heating to high temperatures at each start-up cycle. Moreover, significant energy losses due to heat exchange are possible, which depend on the cell design and size. It is also worth noting the developing direction based on the use of microbial electrolysis cells [318]. Another interesting approach includes a two-step electrochemical–chemical cycle for water splitting [319]. In this process, the hydrogen and oxygen evolution reactions are carried out in different chambers. Low-temperature (25 °C) hydrogen reduction is accompanied by the release of hydroxide ions, which oxidize nickel (II) hydroxide at the anode:

$$Ni(OH)_2 + OH^- - e^- \rightarrow NiOOH + H_2O. \quad (17)$$

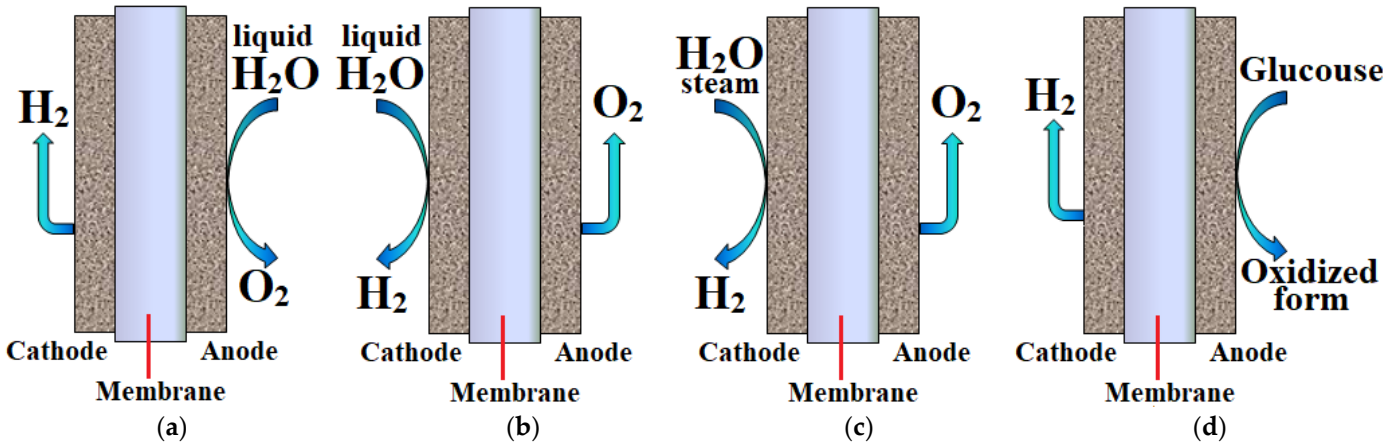

Figure 11. The main types of electrolysis methods: (**a**) proton-exchange membrane water electrolysis; (**b**) alkaline electrolysis; (**c**) high-temperature electrolysis with solid oxide membranes; and (**d**) microbial electrolysis.

Table 4. Comparison of different water electrolysis methods.

Electrolysis Method	Advantages	Disadvantages
Alkaline electrolysis (Commercialized)	- Low cost - High durability - Non-metal electrocatalytic	- Energy efficiency is 70% - Low-purity H_2 - Low operating pressure - Limited current density - Corrosive environment - Gas crossover
Proton-exchange membrane water electrolysis (Good prospects for commercialization)	- Energy efficiency is 80–90% - Ultra-pure H_2 (99.99%) - High operating pressure - High current density - Quick response	- High cost - Acidic environment - Low durability
High-temperature electrolysis with solid oxide membranes (Laboratory scale)	- Energy efficiency is 90–100% - High operating pressure - High current density - Non-metal catalysis	- Large size - Long start-up - Low durability

At the second stage, NiOOH decomposes at an elevated (90 °C) temperature with nickel (II) hydroxide regeneration.

Noble metals (Pt, Pd, Ru, Ir, and Rh) demonstrate excellent catalytic activity in the reaction of hydrogen electroreduction and stability when operating in an electrolyzer [320–322]. To optimize diffusion processes and reduce the noble metal amount, they are usually deposited on supports from nanodispersed carbon materials [323]. Supports based on carbon nanomaterials doped with heteroatoms are also widely used due to their increased conductivity [324,325]. An effective strategy for increasing the activity of catalysts based on noble metals is the formation of alloys or composites with other, more often base, metals or their compounds [326–330]. In this way, the overvoltage of this process can be reduced to 10–50 mV [331].

Transition metal compounds can be used for hydrogen electroreduction instead of platinum-group metals. Thus, the authors of [332,333] concluded that the electronic structure of some transition metal carbides is similar to platinum in many aspects and can exhibit similar catalytic properties. These assumptions were confirmed by Vrubel et al. [334], but the overvoltage of the hydrogen electroreduction reaction turned out to be quite high.

The properties of molybdenum carbide nanostructures turned out to be even more attractive [335]. Phosphides [336] and sulfides of a number of transition metals [337–339] exhibit high catalytic activity in this reaction.

The four-electron oxygen evolution reaction is much more complicated. The following mechanism is currently proposed [305]. In alkaline media, it involves the sorption of hydroxyl ions on catalytic metal centers (M) with electron release (Equation (18)) followed by the formation of oxide centers (M − O) as a result of deprotonation (Equation (19)):

$$OH^- + M \rightarrow M - OH + e^-, \tag{18}$$

$$M - OH + OH^- \rightarrow M - O + H_2O + e^-. \tag{19}$$

Then, oxide centers transform through the formation of peroxide groups (Equations (20) and (21)):

$$M - O + OH^- \rightarrow M - OOH + e^-, \tag{20}$$

$$M - OOH + OH^- \rightarrow O_2 + H_2O + e^- + M \tag{21}$$

or direct formation of an oxygen molecule from two oxide centers:

$$2M - O \rightarrow 2M + O_2. \tag{22}$$

Another mechanism of OER that is also widely discussed in the literature involves the participation of lattice oxygens of catalysts [340–343]. An important step in this mechanism is the formation of oxygen vacancies [344]. Such a mechanism is often suggested for mixed oxides with an oxygen-deficient lattice of the $La_{1-x}Sr_xCoO_{3-\delta}$ type. They generally exhibit high oxygen mobility and rapid oxygen exchange between the gas phase and the lattice. Oxygen vacancies and a mixed oxidation state of these structures also provide fast oxygen transfer in such materials.

The lowest OER overvoltage potentials (about 100–200 mV) were achieved for catalysts based on iridium and ruthenium oxides, which are characterized by an intermediate energy of binding with oxygen-containing radicals [345–349]. The OER rate can be increased by doping these oxides with transition metals. These additives also reduce the catalyst cost [345,350–353]. Among active catalysts, it is also worth noting materials based on platinum [354] and transition metals [355,356] as well as their compounds, including oxides and hydroxides [357,358]. Similar to HER, the use of alloys of platinum and transition metals is effective [354]. Recently, metal–organic frameworks (MOFs) have also been used as catalysts in water electrolysis [359].

At present, the main challenge is to intensify the electrolysis process and make it more efficient [360]. In this way, in addition to improving catalysts properties, the possibility of achieving this through special external force fields is being widely studied. For example, the effect of a supergravity field [361] and ultrasonic action [362] on the performance of electrolytic cells has been studied. The magnetic field application can improve both the mass transfer in the electrolytic cell through increasing the electrolyte convection and the cell performance [363–365]. Jing et al. improved the electrolyzer characteristics through a repetitive, pulsed, high magnetic field [366]. The rate of hydrogen production increased by 15–20% at a magnetic field strength of 10,000 GS [367]. It is important to note that increasing the voltage on the electrolyzer enables the production of hydrogen under high pressure [308], which avoids the energy-consuming stage of hydrogen compression before cylinder filling.

The most widespread PEM electrolyzers contain expensive components such as catalysts based on platinum metals and perfluorinated sulfonic acid membranes. Therefore, the stability of their operation along with a long service life are extremely important issues. A serious problem in electrolysis plants is the degradation of both catalysts and membranes. During the electrolyzer operation, recrystallization of platinum catalyst particles occurs,

resulting in a gradual decrease in the surface area of the catalyst, along with its activity [368]. Moreover, partial dissolution of the catalyst or bipolar plates occurs due to their interaction with a corrosive medium of membranes, which is accompanied by the migration of metal ions incorporated into them by ion-exchange [369,370]. This leads to a significant decrease in the membrane proton conductivity due to a decrease in both the concentration of protons and their mobility. The latter is a result of the so-called "polyalkaline" effect: a decrease in the ion mobility of a compound when there are two types of ions with different mobilities in conduction channels [371]. In this case, the hydrogen crossover leads to a reduction of the metal ions formed due to the catalyst dissolution in the membrane matrix [372,373].

Moreover, an important process is the chemical degradation of membranes [374,375] as the result of the attack of free radicals formed from hydrogen peroxide [376]. In membranes, hydrogen peroxide interacts with dissolved transition metal ions, generating radicals. The same processes also occur when the membrane is treated with the Fenton reagent, which is usually used to study membrane degradation in an accelerated mode [377]:

$$Fe^{2+} + H_2O_2 \rightarrow Fe^{3+} + \bullet OH + OH^-, \quad (23)$$

$$Fe^{3+} + H_2O_2 \rightarrow Fe^{2+} + \bullet OOH + H^+. \quad (24)$$

Most articles report the degradation of perfluorinated sulfonic acid membranes. The radicals formed in these processes attack both side and main perfluorinated chains. The processes with the participation of $–OCF_2$ and C–S bonds, which are most easily attacked by radicals, are characterized by the highest rate. This is accompanied by a decrease in membrane conductivity due to the loss of functional groups [378]. The main chains degrade much more slowly by the gradual elimination of the terminal carboxyl groups. Moreover, membrane degradation is also catalyzed by noble metal nanoparticles deposited in the membrane [376]. In this regard, much attention is paid to the selection of operating conditions of electrolyzers, under which degradation of their components can be minimized [379,380].

In photoelectrolysis of water, water electrolysis occurs using the solar energy absorbed by a semiconductor (usually titania) while applying electric current [381,382].

By using reversible hydrogenases, green microalgae or cyanobacteria are able to direct hydrogen production under special conditions (oxygen-free) in direct biophotolysis while consuming CO_2 [219,383]. In indirect biophotolysis, carbohydrates formed from carbon dioxide at the first step are processed into hydrogen at the next stage [384]. However, the use of this interesting technology is limited by its low efficiency [21,385].

Microbial electrolysis is a relatively new approach to biohydrogen production from organic substances present in biomass, food waste, and/or wastewater [386]. It uses electrochemically active microorganisms (electrogenic bacteria) that oxidize organic matter, generating carbon dioxide, protons, and electrons at the anode. The electrons are then transferred to the cathode to reduce protons, producing hydrogen due to a relatively low (0.2–0.8 V) potential difference [387]. A significant reduction in voltage and total energy consumption compared to classical water electrolysis (in the absence of microorganisms) is achieved due to the fact that the oxidation of water oxygens at the anode is replaced by organic matter oxidation. However, the presence of microorganisms in the solution imposes significant restrictions, such as neutral pH and low salinity of the solution, which causes low electrical conductivity and reduces the hydrogen production efficiency, which hinders microbial electrolysis cell commercial use [387]. One of the trends is the use of membraneless single-chamber microbial electrolysis cells, which also provide high process efficiency [388]. It should be noted that, as well as for other microbial methods of hydrogen production, microbial electrolysis is characterized by low performance and today remains only a promising method for hydrogen production.

Thermochemical water splitting is another promising technology of hydrogen production [389]. Various photoelectrodes are often used to carry out this process more effectively [390], while solar power and nuclear reactors are considered the likely energy

(heat) sources. Today, the construction of such stations requires high costs. This technology is complex, and reports on its effectiveness vary widely.

10. Conclusions

The rapid development of renewable energy and the stochastic nature of its main sources dictate the need for energy storage. The hydrogen cycle is the most promising for mitigation of season fluctuations. According to forecasts, there will be an increase in hydrogen production and a significant redistribution of its application areas, with the electric power industry and transport being the major hydrogen consumers. Comparison of the main hydrogen production processes is given in Table 5.

Table 5. Comparison of the advantages and disadvantages of the main hydrogen production processes.

Process	Advantages	Disadvantages
Steam reforming	Existing infrastructure, low-cost technology	CO and CO_2 emission, high temperatures required, catalyst regeneration required
Partial oxidation	Existing infrastructure, low desulfurization requirement	CO and CO_2 emission, high temperatures required, formation of heavy oils and coke along with H_2, catalyst regeneration required
Auto thermal reforming	Existing infrastructure, developed technology	CO and CO_2 emission, high-purity O_2 required
Biomass gasification	Cheap feedstock, recycling of industrial waste, neutral CO_2 emission, high biomass conversion efficiency	H_2 yield variation due to different biomass compositions, high operating temperatures, seasonal availability
Pyrolysis	Low CO_2 emission	High energy consumption, large carbon amounts, poor fuel efficiency, hydrogen requires deep purification
Electrolysis	CO_2 zero emissions, O_2 is a byproduct, existing infrastructure, high-purity H_2	Expensive

Preference is given to methods that produce high-purity hydrogen without significant emission of carbon oxides. From this point of view, the most promising is water electrolysis using renewable sources. However, the high cost of such hydrogen dictates the need for both its improvement and intensification.

Another promising approach is biomass processing with subsequent hydrogen production from its fermentation products, in particular, bio-alcohols. In this approach, emissions of carbon dioxide during hydrogen production are leveled by its absorption during the biomass cultivation.

At the same time, considerable attention will be paid to the manufacturing of catalysts that can improve the efficiency of hydrogen production, both by advanced and traditional methods. It is noteworthy that many methods of hydrogen production use catalysts of similar composition based on platinum or transition metals and their alloys. This is especially due to the need to activate the C-H bonds in compounds from which hydrogen is produced. In this case, catalysts with an intermediate sorption energy of hydrogen sources exhibit the greatest activity. Increasing attention is also being paid to catalyst supports, which are designed not only to ensure their high dispersion and surface area but also to promote hydrogen production and reduce catalyst poisoning, primarily due to carbon deposition.

One of the promising methods for intensification of high-purity hydrogen production is membrane catalysis using membranes based on palladium alloys. Their unique selectivity produces high-purity hydrogen in a single technological cycle. In this case, the removal of hydrogen from the reaction zone both reduces the process temperature and increases the yield of reaction products in excess of the stoichiometric ones determined by thermodynamics.

Author Contributions: Conceptualization, I.S. and A.Y.; data curation, A.Y.; writing—original draft preparation, I.S. and A.Y.; writing—review and editing, I.S. and A.Y.; funding acquisition, I.S. and A.Y. All authors have read and agreed to the published version of the manuscript.

Funding: This work was supported by the Ministry of Science and Higher Education of the Russian Federation as part of the State Assignment of the Kurnakov Institute of General and Inorganic Chemistry of the Russian Academy of Sciences.

Institutional Review Board Statement: Not applicable.

Informed Consent Statement: Not applicable.

Data Availability Statement: Not applicable.

Conflicts of Interest: The authors declare no conflict of interest.

References

1. Jurasz, J.; Canales, F.A.; Kies, A.; Guezgouz, M.; Beluco, A. A review on the complementarity of renewable energy sources: Concept, metrics, application and future research directions. *Solar Energy* **2020**, *195*, 703–724. [CrossRef]
2. Pagliaro, M.; Meneguzzo, F. Digital management of solar energy en route to energy self-sufficiency. *Glob. Chall.* **2019**, *3*, 1800105. [CrossRef] [PubMed]
3. Kaur, M.; Pal, K. Review on hydrogen storage materials and methods from an electrochemical viewpoint. *J. Energy Storage* **2019**, *23*, 234–249. [CrossRef]
4. Dehghani-Sanij, A.R.; Tharumalingam, E.; Dusseault, M.B.; Fraser, R. Study of energy storage systems and environmental challenges of batteries. *Renew. Sustain. Energy Rev.* **2019**, *104*, 192–208. [CrossRef]
5. Felseghi, R.-A.; Carcadea, E.; Raboaca, M.S.; Trufin, C.N.; Filote, C. Hydrogen Fuel Cell Technology for the Sustainable Future of Stationary Applications. *Energies* **2019**, *12*, 4593. [CrossRef]
6. Staffell, I.; Scamman, D.; Velazquez Abad, A.; Balcombe, P.; Dodds, P.E.; Ekins, P.; Shah, N.; Ward, K.R. The role of hydrogen and fuel cells in the global energy system. *Energy Environ. Sci.* **2019**, *12*, 463–491. [CrossRef]
7. Yaroslavtsev, A.B.; Stenina, I.A.; Golubenko, D.V. Membrane materials for energy production and storage. *Pure Appl. Chem.* **2020**, *92*, 1147–1157. [CrossRef]
8. Song, J.; Wei, C.; Huang, Z.-F.; Liu, C.; Zeng, L.; Wang, X.; Xu, Z.J. A review on fundamentals for designing oxygen evolution electrocatalysts. *Chem. Soc. Rev.* **2020**, *49*, 2196–2214. [CrossRef]
9. Popel', O.S.; Tarasenko, A.B.; Filippov, S.P. Fuel cell based power-generating installations: State of the art and future prospects. *Therm. Eng.* **2018**, *65*, 859–874. [CrossRef]
10. Gielen, D.; Taibi, E.; Miranda, R. *Hydrogen: A Renewable Energy Perspective*; International Renewable Energy Agency: Abu Dhabi, United Arab Emirates, 2019; 52p.
11. Filippov, S.P.; Yaroslavtsev, A.B. Hydrogen energy: Development prospects and materials. *Russ. Chem. Rev.* **2021**, *90*, 627–643. [CrossRef]
12. van Renssen, S. The hydrogen solution? *Nat. Clim. Chang.* **2020**, *10*, 799–801. [CrossRef]
13. *The Future of Hydrogen: Seizing Today's Opportunities*; International Energy Agency: Paris, France, 2019; 200p. Available online: https://read.oecd-ilibrary.org/energy/the-future-of-hydrogen_1e0514c4-en#page7 (accessed on 10 August 2022).
14. *Energy Technology Perspectives*; International Energy Agency: Paris, France, 2020; 398p. Available online: https://iea.blob.core.windows.net/assets/7f8aed40-89af-4348-be19-c8a67df0b9ea/Energy_Technology_Perspectives_2020_PDF.pdf (accessed on 10 August 2022).
15. *Hydrogen Economy Outlook: Key Messages*; Bloomberg Finance L.P.: New York, NY, USA, 2020; 12p. Available online: https://data.bloomberglp.com/professional/sites/24/BNEF-Hydrogen-Economy-Outlook-Key-Messages-30-Mar-2020.pdf (accessed on 10 August 2022).
16. Lesmana, H.; Zhang, Z.; Li, X.; Zhu, M.; Xu, W.; Zhang, D. NH3 as a Transport Fuel in Internal Combustion Engines: A Technical Review. *J. Energy Res. Technol.* **2019**, *141*, 070703. [CrossRef]
17. Oh, S.; Park, C.; Kim, S.; Kim, Y.; Choi, Y.; Kim, C. Natural gas–ammonia dual-fuel combustion in spark-ignited engine with various air–fuel ratios and split ratios of ammonia under part load condition. *Fuel* **2021**, *290*, 120095. [CrossRef]
18. Abe, J.O.; Popoola, A.P.I.; Ajenifuja, E.; Popoola, O.M. Hydrogen energy, economy and storage: Review and recommendation. *Int. J. Hydrogen Energy* **2019**, *44*, 15072–15086. [CrossRef]
19. Parra, D.; Valverde, L.; Pino, F.J.; Patel, M.K. A review on the role, cost and value of hydrogen energy systems for deep decarbonisation. *Renew. Sustain. Energy Rev.* **2019**, *101*, 279–294. [CrossRef]
20. Lee, B.; Heo, J.; Kim, S.; Sung, C.; Moon, C.; Moon, S.; Lim, H. Economic feasibility studies of high pressure PEM water electrolysis for distributed H_2 refueling stations. *Energy Convers. Manag.* **2018**, *162*, 139–144. [CrossRef]
21. Megia, P.J.; Vizcaino, A.J.; Calles, J.A.; Carrero, A. Hydrogen Production Technologies: From Fossil Fuels towards Renewable Sources. A Mini Review. *Energy Fuels* **2021**, *35*, 16403–16415. [CrossRef]

22. Karchiyappan, T.A. Review on hydrogen energy production from electrochemical system: Benefits and challenges. *Energy Sources A* **2019**, *41*, 902–909. [CrossRef]
23. Jiang, L.; Xue, D.; Wei, Z.; Chen, Z.; Mirzayev, M.; Chen, Y.; Chen, S. Coal decarbonization: A state-of-the-art review of enhanced hydrogen production in underground coal gasification. *Energy Rev.* **2022**, *1*, 100004. [CrossRef]
24. Filippov, S.P.; Keiko, A.V. Coal gasification: At the crossroad. Technological Factors. *Therm. Eng.* **2021**, *68*, 209–220. [CrossRef]
25. Jiang, L.; Chen, Z.; Ali Farouq, S.M. Thermal-hydro-chemical-mechanical alteration of coal pores in underground coal gasification. *Fuel* **2020**, *262*, 116543. [CrossRef]
26. Steinberg, M. Fossil fuel decarbonization technology for mitigating global warming. *Int. J. Hydrogen Energy* **1999**, *24*, 771–777. [CrossRef]
27. Rand, D.A.J. A journey on the electrochemical road to sustainability. *J. Solid State Electrochem.* **2011**, *15*, 1579–1622. [CrossRef]
28. Ji, M.; Wang, J. Review and comparison of various hydrogen production methods based on costs and life cycle impact assessment indicators. *Int. J. Hydrogen Energy* **2021**, *46*, 38612–38635. [CrossRef]
29. Abanades, A. Low carbon production of hydrogen by methane decarbonization. In *Production of Hydrogen from Renewable Resources*; Fang, Z., Smith, J.R.L., Qi, X., Eds.; Springer: Dordrecht, The Netherlands, 2015; pp. 149–177.
30. Chi, J.; Yu, H. Water electrolysis based on renewable energy for hydrogen production. *Chin. J. Catal.* **2018**, *39*, 390–394. [CrossRef]
31. Machhammer, O.; Bode, A.; Hormuth, W. Financial and ecological evaluation of hydrogen production processes on large scale. *Chem. Eng. Technol.* **2016**, *39*, 1185–1193. [CrossRef]
32. Pinsky, R.; Sabharwall, P.; Hartvigsen, J.; O'Brien, J. Comparative review of hydrogen production technologies for nuclear hybrid energy systems. *Prog. Nucl. Energy* **2020**, *123*, 103317. [CrossRef]
33. Jokar, S.; Farokhnia, M.A.; Tavakolian, M.; Pejman, M.; Parvasi, P.; Javanmardi, J.; Zare, F.; Gonçalves, M.C.; Basile, A. The recent areas of applicability of palladium based membrane technologies for hydrogen production from methane and natural gas: A review. *Int. J. Hydrogen Energy*, 2022; *in press*. [CrossRef]
34. Iulianelli, A.; Liguori, S.; Wilcox, J.; Basile, A. Advances on methane steam reforming to produce hydrogen through membrane reactors technology: A review. *Catal. Rev.* **2016**, *58*, 1–35. [CrossRef]
35. Chen, L.; Qi, Z.; Zhang, S.; Su, J.; Somorjai, G.A. Catalytic hydrogen production from methane: A review on recent progress and prospect. *Catalysts* **2020**, *10*, 858. [CrossRef]
36. Chen, L.N.; Li, H.Q.; Yan, M.W.; Yuan, C.F.; Zhan, W.W.; Jiang, Y.Q.; Xie, Z.X.; Kuang, Q.; Zheng, L.S. Ternary alloys encapsulated within different MOFs via a self-sacrificing template process: A potential platform for the investigation of size-selective catalytic performances. *Small* **2017**, *13*, 1700683. [CrossRef] [PubMed]
37. Soltani, S.M.; Lahiri, A.; Bahzad, H.; Clough, P.; Gorbounov, M.; Yan, Y. Sorption-enhanced steam methane reforming for combined CO_2 capture and hydrogen production: A State-of-the-Art Review. *Carbon Capture Sci. Technol.* **2021**, *1*, 100003. [CrossRef]
38. Tang, Y.; Wei, Y.; Wang, Z.; Zhang, S.; Li, Y.; Nguyen, L.; Li, Y.; Zhou, Y.; Shen, W.; Tao, F.F.; et al. Synergy of single-atom Ni1 and Ru1 sites on CeO2 for dry reforming of CH_4. *J. Am. Chem. Soc.* **2019**, *141*, 7283–7293. [CrossRef] [PubMed]
39. Song, Y.; Ozdemir, E.; Ramesh, S.; Adishev, A.; Subramanian, S.; Harale, A.; Albuali, M.; Fadhel, B.A.; Jamal, A.; Moon, D.; et al. Dry reforming of methane by stable Ni-Mo nanocatalysts on single-crystalline MgO. *Science* **2020**, *367*, 777–781. [CrossRef]
40. Zhou, L.; Martirez, J.M.P.; Finzel, J.; Zhang, C.; Swearer, D.F.; Tian, S.; Robatjazi, H.; Lou, M.; Dong, L.; Henderson, L.; et al. Light-driven methane dry reforming with single atomic site antenna-reactor plasmonic photocatalysts. *Nat. Energy* **2020**, *5*, 61–70. [CrossRef]
41. Wu, Y.; Pei, C.; Tian, H.; Liu, T.; Zhang, X.; Chen, S.; Xiao, Q.; Wang, X.; Gong, J. Role of Fe Species of Ni-Based Catalysts for Efficient Low-Temperature Ethanol Steam Reforming. *JACS Au* **2021**, *1*, 1459–1470. [CrossRef]
42. Sun, P.; Young, B.; Elgowainy, A.; Lu, Z.; Wang, M.; Morelli, B.; Hawkins, T. Criteria air pollutants and greenhouse gas emissions from hydrogen production in US steam methane reforming facilities. *Environ. Sci. Technol.* **2019**, *53*, 7103–7113. [CrossRef]
43. Vogt, C.; Kranenborg, J.; Monai, M.; Weckhuysen, B.M. Structure sensitivity in steam and dry methane reforming over nickel: Activity and carbon formation. *ACS Catal.* **2019**, *10*, 1428–1438. [CrossRef]
44. Aragao, I.B.; Ro, I.; Liu, Y.; Ball, M.; Huber, G.W.; Zanchet, D.; Dumesic, J.A. Catalysts synthesized by selective deposition of Fe onto Pt for the water-gas shift reaction. *Appl. Catal. B* **2018**, *222*, 182–190. [CrossRef]
45. Mitchell, S.; Perez-Ramirez, J. Single atom catalysis: A decade of stunning progress and the promise for a bright future. *Nat. Commun.* **2020**, *11*, 4302. [CrossRef]
46. Hannagan, R.T.; Giannakakis, G.; Flytzani-Stephanopoulos, M.; Sykes, E.C.H. Single-atom alloy catalysis. *Chem. Rev.* **2020**, *120*, 12044–12088. [CrossRef] [PubMed]
47. Liang, J.-X.; Lin, J.; Liu, J.; Wang, X.; Zhang, T.; Li, J. Dual metal active sites in an Ir1/FeO_x single-atom catalyst: A Redox mechanism for the water-gas shift reaction. *Angew. Chem. Int. Ed.* **2020**, *59*, 12868–12875. [CrossRef] [PubMed]
48. Palma, V.; Ruocco, C.; Cortese, M.; Renda, S.; Meloni, E.; Festa, G.; Martino, M. Platinum based catalysts in the water gas shift reaction: Recent advances. *Metals* **2020**, *10*, 866. [CrossRef]
49. Angeli, S.D.; Turchetti, L.; Monteleone, G.; Lemonidou, A.A. Catalyst development for steam reforming of methane and model biogas at low temperature. *Appl. Catal. B* **2016**, *181*, 34–46. [CrossRef]
50. Wang, J.; Zhang, J.; Zhong, H.; Wang, H.; Ma, K.; Pan, L. Effect of support morphology and size of nickel metal ions on hydrogen production from methane steam reforming. *Chem. Phys. Lett.* **2020**, *746*, 137291. [CrossRef]

51. Lai, G.-H.; Lak, J.H.; Tsai, D.-H. Hydrogen Production via Low-Temperature Steam–Methane Reforming Using Ni–CeO_2–Al_2O_3 Hybrid Nanoparticle Clusters as Catalysts. *ACS Appl. Energy Mater.* **2019**, *2*, 7963–7971. [CrossRef]
52. Sengodan, S.; Lan, R.; Humphreys, J.; Du, D.; Xu, W.; Wang, H.; Tao, S. Advances in reforming and partial oxidation of hydrocarbons for hydrogen production and fuel cell applications. *Renew. Sustain. Energy Rev.* **2018**, *82*, 761–780. [CrossRef]
53. Aghaali, M.H.; Firoozi, S. Enhancing the catalytic performance of Co substituted $NiAl_2O_4$ spinel by ultrasonic spray pyrolysis method for steam and dry reforming of methane. *Int. J. Hydrogen Energy* **2021**, *46*, 357–373. [CrossRef]
54. Kim, D.H.; Youn, J.-R.; Seo, J.-C.; Kim, S.B.; Kim, M.-J.; Lee, K. One-pot synthesis of NiCo/$MgAl_2O_4$ catalyst for high coke-resistance in steam methane reforming: Optimization of Ni/Co ratio. *Catal. Today*, 2022; *in press*. [CrossRef]
55. Santos, D.B.L.; Noronha, F.B.; Hori, C.E. Bi-reforming of methane for hydrogen production using $LaNiO_3/Ce_xZr_{1-x}O_2$ as precursor material. *Int. J. Hydrogen Energy* **2020**, *45*, 13947–13959. [CrossRef]
56. Zhang, H.; Sun, Z.; Hu, Y.H. Steam reforming of methane: Current states of catalyst design and process upgrading. *Renew. Sustain. Energy Rev.* **2021**, *149*, 111330. [CrossRef]
57. Li, R.-j.; Zhang, J.-p.; Shi, J.; Li, K.-z.; Liu, H.-l.; Zhu, X. Regulation of metal-support interface of Ni/CeO_2 catalyst and the performance of low temperature chemical looping dry reforming of methane. *J. Fuel Chem. Technol.* **2022**, *50*, 1458–1470. [CrossRef]
58. Taherian, Z.; Khataee, A.; Han, N.; Orooji, Y. Hydrogen production through methane reforming processes using promoted-Ni/mesoporous silica: A review. *J. Ind. Eng. Chem.* **2022**, *107*, 20–30. [CrossRef]
59. Zuo, Z.; Liu, S.; Wang, Z.; Liu, C.; Huang, W.; Huang, J.; Liu, P. Dry reforming of methane on single-site Ni/MgO catalysts: Importance of site confinement. *ACS Catal.* **2018**, *8*, 9821–9835. [CrossRef]
60. Huang, J.; Liu, W.; Yang, Y.; Liu, B. High-performance Ni–Fe redox catalysts for selective CH_4 to syngas conversion via chemical looping. *ACS Catal.* **2018**, *8*, 1748–1756. [CrossRef]
61. Meloni, E.; Martino, M.; Palma, V. A short review on Ni based catalysts and related engineering issues for methane steam reforming. *Catalysts* **2020**, *10*, 352. [CrossRef]
62. Dou, B.; Wang, C.; Song, Y.; Chen, H.; Jiang, B.; Yang, M.; Xu, Y. Solid sorbents for in-situ CO_2 removal during sorption-enhanced steam reforming process: A review. *Renew. Sustain. Energy Rev.* **2016**, *53*, 536–546. [CrossRef]
63. Yan, Y.; Manovic, V.; Anthony, E.J.; Clough, P.T. Techno-economic analysis of low-carbon hydrogen production by sorption enhanced steam methane reforming (SE-SMR) processes. *Energy Convers. Manag.* **2020**, *226*, 113530. [CrossRef]
64. Nkulikiyinka, P.; Yan, Y.; Gulec, F.; Manovic, V.; Clough, P.T. Prediction of sorption enhanced steam methane reforming products from machine learning based soft-sensor models. *Energy AI* **2020**, *2*, 100037. [CrossRef]
65. Alent'ev, A.Y.; Volkov, A.V.; Vorotyntsev, I.V.; Maksimov, A.L.; Yaroslavtsev, A.B. Membrane Technologies for Decarbonization. *Membr. Membr. Technol.* **2021**, *3*, 255–273. [CrossRef]
66. Zhao, C.; Zhou, Z.; Cheng, Z.; Fang, X. Sol-gel-derived, $CaZrO_3$-stabilized Ni/CaO-$CaZrO_3$ bifunctional catalyst for sorption-enhanced steam methane reforming. *Appl. Catal. B* **2016**, *196*, 16–26. [CrossRef]
67. Papalas, T.; Antzaras, A.N.; Lemonidou, A.A. Intensified steam methane reforming coupled with Ca-Ni looping in a dual fluidized bed reactor system: A conceptual design. *Chem. Eng. J.* **2020**, *382*, 122993. [CrossRef]
68. Wang, M.; Wang, G.; Sun, Z.; Zhang, Y.; Xu, D. Review of renewable energy-based hydrogen production processes for sustainable energy innovation. *Glob. Energy Intercon.* **2019**, *2*, 436–443. [CrossRef]
69. Liu, F.Q.; Li, G.-H.; Luo, S.-W.; Li, W.-H.; Huang, Z.-G.; Li, W.; Su, F.; Li, C.-Q.; Ding, Z.-B.; Jiang, Q. Ultrafast carbon dioxide sorption kinetics using morphology controllable lithium zirconate. *ACS Appl. Mater. Interfaces* **2019**, *11*, 691–698. [CrossRef] [PubMed]
70. Munro, S.; Ahlen, M.; Cheung, O.; Sanna, A. Tuning Na_2ZrO_3 for fast and stable CO_2 adsorption by solid state synthesis. *Chem. Eng. J.* **2020**, *388*, 124284. [CrossRef]
71. Wang, Y.; Memon, M.Z.; AliSeelro, M.; Fu, W.; Gao, Y.; Dong, Y.; Ji, G. A review of CO_2 sorbents for promoting hydrogen production in the sorption-enhanced steam reforming process. *Int. J. Hydrogen Energy* **2021**, *46*, 23358–23379. [CrossRef]
72. Schwartz, N.; Harrington, J.; Ziegler, K.; Cox, P. Effects of structure and chemistry on electrochemical transport properties of anion exchange membranes for separation of CO_2. *Sep. Sci. Technol.* **2023**, *58*, 212–219. [CrossRef]
73. di Giuliano, A.; Gallucci, K. Sorption enhanced steam methane reforming based on nickel and calcium looping: A review. *Chem. Eng. Process.* **2018**, *130*, 240–252. [CrossRef]
74. Cherbanski, R.; Molga, E. Sorption-enhanced steam methane reforming (SE-SMR)—A review: Reactor types, catalyst and sorbent characterization, process modeling. *Chem. Process Eng.* **2018**, *39*, 427–448.
75. Osman, A.I. Catalytic hydrogen production from methane partial oxidation: Mechanism and kinetic study. *Chem. Eng. Technol.* **2020**, *43*, 641–648. [CrossRef]
76. Alvarez-Galvan, C.; Melian, M.; Ruiz-Matas, L.; Eslava, J.L.; Navarro, R.M.; Ahmadi, M.; Cuenya, B.R.; Fierro, J.L.G. Partial oxidation of methane to syngas over nickel-based catalysts: Influence of support type, addition of rhodium, and preparation method. *Front. Chem.* **2019**, *7*, 104. [CrossRef] [PubMed]
77. Li, L.; MD Dostagir, N.H.; Shrotri, A.; Fukuoka, A.; Kobayashi, H. Partial oxidation of methane to syngas via formate Intermediate found for a ruthenium–rhenium bimetallic catalyst. *ACS Catal.* **2021**, *11*, 3782–3789. [CrossRef]
78. Alhassan, M.; Jalil, A.A.; Nabgan, W.; Hamid, M.Y.S.; Bahari, M.B.; Ikram, M. Bibliometric studies and impediments to valorization of dry reforming of methane for hydrogen production. *Fuel* **2022**, *328*, 125240. [CrossRef]

79. Ma, Y.; Ma, Y.; Long, G.; Li, J.; Hu, X.; Ye, Z.; Wang, Z.; Buckley, C.E.; Dong, D. Synergistic promotion effect of MgO and CeO_2 on nanofibrous Ni/Al_2O_3 catalysts for methane partial oxidation. *Fuel* **2019**, *258*, 116103. [CrossRef]
80. Enger, B.C.; Lødeng, R.; Holmen, A. A review of catalytic partial oxidation of methane to synthesis gas with emphasis on reaction mechanisms over transition metal catalysts. *Appl. Catal. A* **2018**, *346*, 1–27. [CrossRef]
81. Moiseev, I.I.; Loktev, A.S.; Shlyakhtin, O.A.; Mazo, G.N.; Dedov, A.G. New approaches to the design of nickel, cobalt, and Nickel–cobalt catalysts for partial oxidation and dry reforming of methane to synthesis gas. *Petr. Chem.* **2019**, *59*, S1–S20. [CrossRef]
82. Ha, Q.L.M.; Lund, H.; Kreyenschulte, C.; Bartling, S.; Atia, H.; Vuong, T.H.; Wohlrab, S.; Armbruster, U. Development of highly stable Low Ni content catalyst for dry reforming of CH_4-rich feedstocks. *ChemCatChem* **2020**, *12*, 1562–1568. [CrossRef]
83. Moral, A.; Reyero, I.; Llorc, J.; Bimbela, F.; Gandía, L.M. Partial oxidation of methane to syngas using Co/Mg and Co/Mg-Al oxide supported catalysts. *Catal. Today* **2019**, *333*, 259–267. [CrossRef]
84. Khatun, R.; Bhandari, S.; Poddar, M.K.; Samanta, C.; Khan, T.S.; Khurana, D.; Bal, R. Partial oxidation of methane over high coke-resistant bimetallic Pt-Ni/CeO_2 catalyst: Profound influence of Pt addition on stability. *Int. J. Hydrogen Energy* **2022**, *47*, 38895–38909. [CrossRef]
85. Wachter, P.; Hödl, P.; Raic, J.; Gaber, C.; Demuth, M.; Hochenauer, C. Towards thermochemical recuperation applying combined steam reforming and partial oxidation of methane: Thermodynamic and experimental considerations. *Energy Convers. Manag.* **2022**, *251*, 114927. [CrossRef]
86. Pal, D.B.; Chand, R.; Upadhyay, S.N.; Mishra, P.K. Performance of water gas shift reaction catalysts: A review. *Renew. Sustain. Energy Rev.* **2018**, *93*, 549–565. [CrossRef]
87. Ebrahimi, P.; Kumar, A.; Khraisheh, M. A review of recent advances in water-gas shift catalysis for hydrogen production. *Emergent Mater.* **2020**, *3*, 881–917. [CrossRef]
88. Uvarov, V.I.; Kapustin, R.D.; Fedotov, A.S.; Kirillov, A.O. Synthesis of porous ceramic materials for catalytically active membranes by technological combustion and sintering. *Glass Ceram.* **2020**, *77*, 221–225. [CrossRef]
89. Dan, M.; Mihet, M.; Borodi, G.; Lazar, M.D. Combined steam and dry reforming of methane for syngas production from biogas using bimodal pore catalysts. *Catal. Today* **2021**, *366*, 87–96. [CrossRef]
90. Guilhaume, N.; Bianchi, D.; Wandawa, R.A.; Yin, W.; Schuurman, Y. Study of CO_2 and H_2O adsorption competition in the combined dry / steam reforming of biogas. *Catal. Today* **2021**, *375*, 282–289. [CrossRef]
91. Osman, A.I.; Abu-Dahrieh, J.K.; Laffir, F.; Curtin, T.; Thompson, J.M.; Rooney, D.W. A bimetallic catalyst on a dual component support for low temperature total methane oxidation. *Appl. Catal. B* **2016**, *187*, 408–418. [CrossRef]
92. Osman, A.I.; Abu-Dahrieh, J.K.; McLaren, M.; Laffir, F.; Rooney, D.W. Characterisation of robust combustion catalyst from aluminium foil waste. *Chem. Select* **2018**, *3*, 1545–1550. [CrossRef]
93. Ren, S.; Zhang, Y.; Liu, Y.; Sakao, T.; Huisingh, D.; Almeida, C.M.V.B. A comprehensive review of big data analytics throughout product lifecycle to support sustainable smart manufacturing: A framework, challenges and future research directions. *J. Clean. Prod.* **2019**, *210*, 1343–1365. [CrossRef]
94. Leclerc, C.A.; Gudgila, R. Short Contact Time Catalytic Partial Oxidation of Methane over Rhodium Supported on Ceria Based 3-D Printed Supports. *Ind. Eng. Chem. Res.* **2019**, *58*, 14632–14637. [CrossRef]
95. Siang, T.J.; Jalil, A.A.; Liew, S.Y.; Owgi, A.H.K.; Rahman, A.F.A. A review on state-of-the-art catalysts for methane partial oxidation to syngas production. *Catal. Rev.* **2022**, *11*, 1–57. [CrossRef]
96. Ren, Y.; Yang, Y.; Zhao, Y.-X.; He, S.-G. Conversion of Methane with Oxygen to Produce Hydrogen Catalyzed by Triatomic Rh3–Cluster Anion. *J. Am. Chem. Soc.* **2022**, *2*, 197–203. [CrossRef] [PubMed]
97. Boukha, Z.; Gil-Calvo, M.; de Rivas, B.; Gonzalez-Velasco, J.R.; Gutierrez-Ortiz, J.I.; Lopez-Fonseca, R. Behaviour of Rh supported on hydroxyapatite catalysts in partial oxidation and steam reforming of methane: On the role of the speciation of the Rh particles. *Appl. Catal. A* **2018**, *556*, 191–203. [CrossRef]
98. Cheephat, C.; Daorattanachai, P.; Devahastin, S.; Laosiripojana, N. Partial oxidation of methane over monometallic and bimetallic Ni-, Rh-, Re-based catalysts: Effects of Re addition, co-fed reactants and catalyst support. *Appl. Catal. A* **2018**, *563*, 1–8. [CrossRef]
99. Rogozhnikov, V.N.; Snytnikov, P.V.; Salanov, A.N.; Kulikov, A.V.; Ruban, N.V.; Potemkin, D.I.; Sobyanin, V.A.; Kharton, V.V. Rh/θ-Al_2O_3/FeCrAlloy wire mesh composite catalyst for partial oxidation of natural gas. *Mater. Lett.* **2019**, *236*, 316–319. [CrossRef]
100. Ding, C.; Wang, J.; Guo, S.; Ma, Z.; Li, Y.; Ma, L.; Zhang, K. Abundant hydrogen production over well dispersed nickel nanoparticles confined in mesoporous metal oxides in partial oxidation of methane. *Int. J. Hydrogen Energy* **2019**, *44*, 30171–30184. [CrossRef]
101. Dossumov, K.; Kurokawa, H.; Yergaziyeva, Y.; Myltykbayeva, L.; Tayrabekova, S. Nickel Oxide Catalysts for Partial Oxidation of Methane to Synthesis Gas. *Eurasian Chem.-Technol. J.* **2016**, *18*, 25–30. [CrossRef]
102. Choudhary, V.R.; Mondal, K.C.; Choudhary, T.V. Partial oxidation of methane to syngas with or without simultaneous steam or CO_2 reforming over a high-temperature stable-NiCoMgCeO_x supported on zirconia–hafnia catalyst. *Appl. Catal. A* **2016**, *306*, 45–50. [CrossRef]
103. Karaismailoglu, M.; Figen, H.E.; Baykara, S.Z. Hydrogen production by catalytic methane decomposition over yttria doped nickel based catalysts. *Int. J. Hydrogen Energy* **2019**, *44*, 9922–9929. [CrossRef]

104. Osman, A.I.; Meudal, J.; Laffir, F.; Thompson, J.; Rooney, D. Enhanced catalytic activity of Ni on η-Al_2O_3 and ZSM-5 on addition of ceria zirconia for the partial oxidation of methane. *Appl. Catal. B* **2017**, *212*, 68–79. [CrossRef]
105. Alam, S.; Kumar, J.P.; Rani, K.Y.; Sumana, C. Self-sustained process scheme for high purity hydrogen production using sorption enhanced steam methane reforming coupled with chemical looping combustion. *J. Clean. Prod.* **2017**, *162*, 687–701. [CrossRef]
106. Yan, Y.; Thanganadar, D.; Clough, P.T.; Mukherjee, S.; Patchigolla, K.; Manovic, V.; Anthony, E.J. Process simulations of blue hydrogen production by upgraded sorption enhanced steam methane reforming (SE-SMR) processes. *Energy Convers. Manag.* **2020**, *222*, 113144. [CrossRef]
107. Saithong, N.; Authayanun, S.; Patcharavorachot, Y.; Arpornwichanop, A. Thermodynamic analysis of the novel chemical looping process for two-grade hydrogen production with CO_2 capture. *Energy Convers. Manag.* **2019**, *180*, 325–337. [CrossRef]
108. Wang, Y.; Yao, L.; Wang, Y.; Wang, S.; Zhao, Q.; Mao, D.; Hu, C. Low-temperature catalytic CO_2 dry reforming of methane on Ni-Si/ZrO_2 catalyst. *ACS Catal.* **2018**, *8*, 6495–6506. [CrossRef]
109. Nedolivko, V.V.; Zasypalov, G.O.; Vutolkina, A.V.; Gushchin, P.A.; Vinokurov, V.A.; Kulikov, L.A.; Egazar'yants, S.V.; Karakhanov, E.A.; Maksimov, A.L.; Glotov, A.P. Carbon dioxide reforming of methane. *Russ. J. Appl. Chem.* **2020**, *93*, 765–787. [CrossRef]
110. Aramouni, N.A.K.; Touma, J.G.; Tarboush, B.A.; Zeaiter, J.; Ahmad, M.N. Catalyst design for dry reforming of methane: Analysis review. *Renew. Sustain. Energy Rev.* **2018**, *82*, 2570–2585. [CrossRef]
111. Chen, L.; Gangadharan, P.; Lou, H.H. Sustainability assessment of combined steam and dry reforming versus tri-reforming of methane for syngas production. *Asia-Pac. J. Chem. Eng.* **2018**, *13*, e2168. [CrossRef]
112. Wittich, K.; Krämer, M.; Bottke, N.; Schunk, S.A. Catalytic Dry Reforming of Methane: Insights from Model Systems. *ChemCatChem* **2020**, *12*, 2130–2147. [CrossRef]
113. Rosli, S.N.A.; Abidin, S.Z.; Osazuwa, O.U.; Fan, X.; Jiao, Y. The effect of oxygen mobility/vacancy on carbon gasification in nano catalytic dry reforming of methane: A review. *J. CO2 Util.* **2022**, *63*, 102109. [CrossRef]
114. Niu, J.; Guo, F.; Ran, J.; Qi, W.; Yang, Z. Methane dry (CO_2) reforming to syngas (H_2/CO) in catalytic process: From experimental study and DFT calculations. *Int. J. Hydrogen Energy* **2020**, *45*, 30267–30287. [CrossRef]
115. Gamal, A.; Eid, K.; Abdullah, A.M. Engineering of Pt-based nanostructures for efficient dry (CO_2) reforming: Strategy and mechanism for rich-hydrogen production. *Int. J. Hydrogen Energy* **2022**, *47*, 5901–5928. [CrossRef]
116. Fedotov, A.S.; Tsodikov, M.V.; Yaroslavtsev, A.B. Hydrogen Production in Catalytic Membrane Reactors Based on Porous Ceramic Converters. *Processes* **2022**, *10*, 2060. [CrossRef]
117. Li, X.; Li, D.; Tian, H.; Zeng, L.; Zhao, Z.J.; Gong, J. Dry reforming of methane over Ni/La_2O_3 nanorod catalysts with stabilized Ni nanoparticles. *Appl. Catal. B.* **2017**, *202*, 683–694. [CrossRef]
118. Bakhtiari, K.; Kootenaei, A.S.; Maghsoodi, S.; Azizi, S.; Ghomsheh, S.M.T. Synthesis of high sintering-resistant Ni-modified halloysite based catalysts containing La, Ce, and Co for dry reforming of methane. *Ceram. Int.* **2022**, *48*, 37394–37402. [CrossRef]
119. Zeng, F.; Zhang, J.; Xu, R.; Zhang, R.; Ge, J. Highly dispersed Ni/MgO-mSiO_2 catalysts with excellent activity and stability for dry reforming of methane. *Nano Res.* **2022**, *15*, 5004–5013. [CrossRef]
120. Salaev, M.A.; Liotta, L.F.; Vodyankina, O.V. Lanthanoid-containing Ni-based catalysts for dry reforming of methane: A review. *Int. J. Hydrogen Energy* **2022**, *47*, 4489–4535. [CrossRef]
121. Li, K.; Chang, X.; Pei, C.; Li, X.; Chen, S.; Zhang, X.; Assabumrungrat, S.; Zhao, Z.-J.; Zeng, L.; Gong, J. Ordered mesoporous Ni/La_2O_3 catalysts with interfacial synergism towards CO_2 activation in dry reforming of methane. *Appl. Catal. B* **2019**, *259*, 118092. [CrossRef]
122. La Parola, V.; Liotta, L.F.; Pantaleo, G.; Testa, M.L.; Venezia, A.M. CO_2 reforming of CH_4 over Ni supported on SiO_2 modified by TiO_2 and ZrO_2: Effect of the support synthesis procedure. *Appl. Catal. A* **2022**, *642*, 118704. [CrossRef]
123. Li, L.; Chen, J.; Zhang, Q.; Yang, Z.; Sun, Y.; Zou, G. Methane dry reforming over activated carbon supported Ni-catalysts prepared by solid phase synthesis. *J. Clean. Prod.* **2020**, *274*, 122256. [CrossRef]
124. Zhang, R.; Xia, G.; Li, M.; Wu, Y.; Nie, H.; Li, D. Effect of support on the performance of Ni-based catalyst in methane dry reforming. *J. Fuel Chem. Technol.* **2015**, *43*, 1359–1365. [CrossRef]
125. Han, J.W.; Park, J.S.; Choi, M.S.; Lee, H. Uncoupling the size and support effects of Ni catalysts for dry reforming of methane. *Appl. Catal. B* **2017**, *203*, 625–632. [CrossRef]
126. Pizzolitto, C.; Pupulin, E.; Menegazzo, F.; Ghedini, E.; Di Michele, A.; Mattarelli, M.; Cruciani, G.; Signoretto, M. Nickel based catalysts for methane dry reforming. Effect of supports on catalytic activity and stability. *Int. J. Hydrogen Energy* **2019**, *44*, 28065–28076. [CrossRef]
127. Bukhari, S.N.; Chin, C.Y.; Setiabudi, H.D.; Vo, D.V.N. Tailoring the properties and catalytic activities of Ni/SBA-15 via different TEOS/P123 mass ratios for CO_2 reforming of CH_4. *J. Environ. Chem. Eng.* **2017**, *5*, 3122–3128. [CrossRef]
128. Wang, X.; Xu, S.; Yang, W.; Fan, X.; Pan, Q.; Chen, H. Development of Ni-Co supported on SBA-15 catalysts for non-thermal plasma assisted co-conversion of CO_2 and CH_4: Results and lessons learnt. *Carbon Capture Sci. Technol.* **2022**, *5*, 100067. [CrossRef]
129. Kiani, P.; Meshksar, M.; Rahimpour, M.R.; Iulianelli, A. CO_2 utilization in methane reforming using La-doped SBA-16 catalysts prepared via pH adjustment method. *Fuel* **2022**, *322*, 124248. [CrossRef]
130. Valderrama, G.; Urbina De Navarro, C.; Goldwasser, M.R. CO_2 reforming of CH_4 over Co-La-based perovskite-type catalyst precursors. *J. Power Source* **2013**, *234*, 31–37. [CrossRef]
131. Sánchez-Bastardo, N.; Schlögl, R.; Ruland, H. Methane pyrolysis for CO_2-free H_2 production: A green process to overcome renewable energies unsteadiness. *Chem. Ing. Tech.* **2020**, *92*, 1596–1609. [CrossRef]

132. Pinaeva, L.G.; Noskov, A.S.; Parmon, V.N. Prospects for the direct catalytic conversion of methane into useful chemical products. *Catal. Ind.* **2017**, *9*, 283–298. [CrossRef]
133. Parfenov, V.E.; Nikitchenko, N.V.; Pimenov, A.A.; Kuz'min, A.E.; Kulikova, M.V.; Chupichev, O.B.; Maksimov, A.L. Methane pyrolysis for hydrogen production: Specific features of using molten metals. *Russ. J. Appl. Chem.* **2020**, *93*, 625–632. [CrossRef]
134. Naikoo, G.A.; Arshad, F.; Hassan, I.U.; Tabook, M.A.; Pedram, M.Z.; Mustaqeem, M.; Tabassum, H.; Ahmed, W.; Rezakazemi, M. Thermocatalytic hydrogen production through decomposition of methane. A review. *Front. Chem.* **2021**, *9*, 736801. [CrossRef]
135. Weger, L.; Abánades, A.; Butler, T. Methane cracking as a bridge technology to the hydrogen economy. *Int. J. Hydrogen Energy* **2017**, *42*, 720–731. [CrossRef]
136. Qian, J.X.; Chen, T.W.; Enakonda, L.R.; Liu, D.B.; Mignani, G.; Basset, J.M.; Zhou, L. Methane decomposition to produce COx-free hydrogen and nano-carbon over metal catalysts: A review. *Int. J. Hydrogen Energy* **2020**, *45*, 7981–8001. [CrossRef]
137. Sanchez-Bastardo, N.; Schlögl, R.; Ruland, H. Methane pyrolysis for zero-emission hydrogen production: A potential bridge technology from fossil fuels to a renewable and sustainable hydrogen economy. *Ind. Eng. Chem. Res.* **2021**, *60*, 11855–11881. [CrossRef]
138. Banu, A.; Bicer, Y. Integration of methane cracking and direct carbon fuel cell with CO_2 capture for hydrogen carrier production. *Int. J. Hydrogen Energy* **2022**, *47*, 19502–19516. [CrossRef]
139. Korányi, T.I.; Németh, M.; Beck, A.; Horváth, A. Recent Advances in Methane Pyrolysis: Turquoise Hydrogen with Solid Carbon Production. *Energies* **2022**, *15*, 6342. [CrossRef]
140. Saraswat, S.K.; Sinha, B.; Pant, K.K.; Gupta, R.B. Kinetic study and modeling of homogeneous thermocatalytic decomposition of methane over a $Ni-Cu-Zn/Al_2O_3$ catalyst for the production of hydrogen and bamboo-shaped carbon nanotubes. *Ind. Eng. Chem. Res.* **2016**, *55*, 11672–11680. [CrossRef]
141. Yadav, M.D.; Patwardhan, A.W.; Joshi, J.B.; Dasgupta, K. Kinetic study of multi-walled carbon nanotube synthesis by thermocatalytic decomposition of methane using floating catalyst chemical vapour deposition. *Chem. Eng. J.* **2019**, *377*, 119895. [CrossRef]
142. Wang, J.; Li, X.; Zhou, Y.; Yu, G.; Jin, L.; Hu, H. Mechanism of methane decomposition with hydrogen addition over activated carbon via in-situ pyrolysis-electron impact ionization time-of-flight mass spectrometry. *Fuel* **2020**, *263*, 116734. [CrossRef]
143. Chen, Q.; Lua, A.C. Kinetic reaction and deactivation studies on thermocatalytic decomposition of methane by electroless nickel plating catalyst. *Chem. Eng. J.* **2020**, *389*, 124366. [CrossRef]
144. Bayat, N.; Rezaei, M.; Meshkani, F. Hydrogen and carbon nanofibers synthesis by methane decomposition over $Ni\text{-}Pd/Al_2O_3$ catalyst. *Int. J. Hydrogen Energy* **2016**, *41*, 5494–5503. [CrossRef]
145. Pudukudy, M.; Yaakob, Z.; Jia, Q.M.; Takriff, M.S. Catalytic decomposition of undiluted methane into hydrogen and carbon nanotubes over Pt promoted Ni/CeO_2 catalysts. *New J. Chem.* **2018**, *42*, 14843–14856. [CrossRef]
146. Kutteri, D.A.; Wang, I.-W.; Samanta, A.; Li, L.L.; Hu, J.L. Methane decomposition to tip and base grown carbon nanotubes and CO_x-free H_2 over mono- and bimetallic 3d transition metal catalysts. *Catal. Sci. Technol.* **2018**, *8*, 858–869. [CrossRef]
147. Fakeeha, A.H.; Ibrahim, A.A.; Khan, W.U.; Seshan, K.; AlOtaibi, R.L.; Al-Fatesh, A.S. Hydrogen production via catalytic methane decomposition over alumina supported iron catalyst. *Arab. J. Chem.* **2018**, *11*, 405–414. [CrossRef]
148. Rastegarpanah, A.; Rezaei, M.; Meshkani, F.; Zhang, K.F.; Zhao, X.T.; Pei, W.B.; Liu, Y.X.; Deng, J.G.; Arandiyan, H.; Dai, H.X. Mesoporous Ni/MeO_x (Me = Al, Mg, Ti, and Si): Highly efficient catalysts in the decomposition of methane for hydrogen production. *Appl. Surf. Sci.* **2019**, *478*, 581–593. [CrossRef]
149. Wang, D.; Zhang, J.; Sun, J.B.; Gao, W.M.; Cui, Y.B. Effect of metal additives on the catalytic performance of Ni/Al_2O_3 catalyst in thermocatalytic decomposition of methane. *Int. J. Hydrogen Energy* **2019**, *44*, 7205–7215. [CrossRef]
150. Ouyang, M.Z.; Boldrin, P.; Maher, R.C.; Chen, X.L.; Liu, X.H.; Cohen, L.F.; Brandon, N.P. A mechanistic study of the interactions between methane and nickel supported on doped ceria. *Appl. Catal. B* **2019**, *248*, 332–340. [CrossRef]
151. Wang, J.F.; Jin, L.J.; Li, Y.; Hu, H.Q. Preparation of Fedoped carbon catalyst for methane decomposition to hydrogen. *Ind. Eng. Chem. Res.* **2017**, *56*, 11021–11027. [CrossRef]
152. Ibrahim, A.A.; Fakeeha, A.H.; Al-Fatesh, A.S.; Abasaeed, A.E.; Khan, W.U. Methane decomposition over iron catalyst for hydrogen production. *Int. J. Hydrogen Energy* **2015**, *40*, 7593–7600. [CrossRef]
153. Wang, I.-W.; Kutteri, D.A.; Gao, B.Y.; Tian, H.J.; Hu, J.L. Methane pyrolysis for carbon nanotubes and COx-free H_2 over transition-metal catalysts. *Energy Fuels* **2019**, *33*, 197–205. [CrossRef]
154. Pudukudy, M.; Yaakob, Z. Methane decomposition over Ni, Co and Fe based monometallic catalysts supported on sol gel derived SiO_2 microflakes. *Chem. Eng. J.* **2015**, *262*, 1009–1021. [CrossRef]
155. Silva, R.R.C.M.; Oliveira, H.A.; Guarino, A.C.P.F.; Toledo, B.B.; Moura, M.B.T.; Oliveira, B.T.M.; Passos, F.B. Effect of support on methane decomposition for hydrogen production over cobalt catalysts. *Int. J. Hydrogen Energy* **2016**, *41*, 6763–6772. [CrossRef]
156. Pudukudy, M.; Yaakob, Z.; Kadier, A.; Takriff, M.S.; Hassan, N.S.M. One-pot sol–gel synthesis of Ni/TiO_2 catalysts for methane decomposition into COx free hydrogen and multiwalled carbon nanotubes. *Int. J. Hydrogen Energy* **2017**, *42*, 16495–16513. [CrossRef]
157. Garcia-Sancho, C.; Guil-López, R.; Sebastian-Lopez, A.; Navarro, R.M.; Fierro, J.L.G. Hydrogen production by methane decomposition: A comparative study of supported and bulk ex-hydrotalcite mixed oxide catalysts with Ni, Mg and Al. *Int. J. Hydrogen Energy* **2018**, *43*, 9607–9621. [CrossRef]

158. Al-Fatesh, A.S.; Barama, S.; Ibrahim, A.A.; Barama, A.; Khan, W.U.; Fakeeha, A. Study of methane decomposition on Fe/MgO-based catalyst modified by Ni, Co, and Mn additives. *Chem. Eng. Commun.* **2017**, *204*, 739–749. [CrossRef]
159. Rastegarpanah, A.; Meshkani, F.; Rezaei, M. Thermocatalytic decomposition of methane over mesoporous nanocrystalline promoted Ni/MgO•Al_2O_3 catalysts. *Int. J. Hydrogen Energy* **2017**, *42*, 16476–16488. [CrossRef]
160. Torres, D.; Pinilla, J.L.; Suelves, I. Co-, Cu- and Fe-doped Ni/Al_2O_3 catalysts for the catalytic decomposition of methane into hydrogen and carbon nanofibers. *Catalysts* **2018**, *8*, 300. [CrossRef]
161. Torres, D.; Pinilla, J.L.; Suelves, I. Screening of Ni-Cu bimetallic catalysts for hydrogen and carbon nanofilaments production via catalytic decomposition of methane. *Appl. Catal. A* **2018**, *559*, 10–19. [CrossRef]
162. Ashik, U.P.M.; Abbas, H.F.; Abnis, F.; Kudo, S.; Hayashi, J.-I.; Wan Daud, W.M.A. Methane decomposition with a minimal catalyst: An optimization study with response surface methodology over Ni/SiO_2 nanocatalyst. *Int. J. Hydrogen Energy* **2020**, *45*, 14383–14395. [CrossRef]
163. Rategarpanah, A.; Meshkani, F.; Wang, Y.; Arandiyan, H.; Rezaei, M. Thermocatalytic conversion of methane to highly pure hydrogen over Ni–Cu/MgO·Al_2O_3catalysts: Influence of noble metals (Pt and Pd) on the catalytic activity and stability. *Energy Convers. Manag.* **2018**, *166*, 268–280. [CrossRef]
164. Khan, W.U.; Fakeeha, A.H.; Al-Fatesh, A.S.; Ibrahim, A.A.; Abasaeed, A.E. La_2O_3 supported bimetallic catalysts for the production of hydrogen and carbon nanomaterials from methane. *Int. J. Hydrogen Energy* **2016**, *41*, 976–983. [CrossRef]
165. Bayat, N.; Rezaei, M.; Meshkani, F. Methane decomposition over Ni-Fe/Al_2O_3 catalysts for production of CO_x-free hydrogen and carbon nanofiber. *Int. J. Hydrogen Energy* **2016**, *41*, 1574–1584. [CrossRef]
166. Al-Mubaddel, F.; Kasim, S.; Ibrahim, A.A.; Al-Awadi, A.S.; Fakeeha, A.H.; Al-Fatesh, A.S. H_2 Production from Catalytic Methane Decomposition Using Fe/x-ZrO_2 and Fe-Ni/(x-ZrO_2) (x = 0, La_2O_3, WO_3) Catalysts. *Catalysts* **2020**, *10*, 793. [CrossRef]
167. Torres, D.; Pinilla, J.L.; L'azaro, M.J.; Moliner, R.; Suelves, I. Hydrogen and multiwall carbon nanotubes production by catalytic decomposition of methane: Thermogravimetric analysis and scaling-up of Fe-Mo catalysts. *Int. J. Hydrogen Energy* **2014**, *39*, 3698–3709. [CrossRef]
168. Zhou, L.; Enakonda, L.R.; Harb, M.; Saih, Y.; Aguilar-Tapia, A.; Ould-Chikh, S.; Hazemann, J.-l.; Li, J.; Wei, N.; Gary, D.; et al. Fe catalysts for methane decomposition to produce hydrogen and carbon nano materials. *Appl. Catal. B* **2017**, *208*, 44–59. [CrossRef]
169. Vlaskin, M.S.; Grigorenko, A.V.; Gromov, A.A.; Kumar, V.; Dudoladov, A.O.; Slavkina, O.V.; Darishchev, V.I. Methane pyrolysis on sponge iron powder for sustainable hydrogen production. *Res. Eng.* **2022**, *15*, 100598. [CrossRef]
170. Zhang, J.; Li, X.; Chen, H.; Qi, M.; Zhang, G.; Hu, H.; Ma, X. Hydrogen production by catalytic methane decomposition: Carbon materials as catalysts or catalyst supports. *Int. J. Hydrogen Energy* **2017**, *42*, 19755–19775. [CrossRef]
171. Zhang, J.B.; Li, X.; Xie, W.T.; Hao, Q.Q.; Chen, H.Y.; Ma, X. K_2CO_3-promoted methane pyrolysis on nickel/coal-char hybrids. *J. Anal. Appl. Pyrolysis* **2018**, *136*, 53–61. [CrossRef]
172. Patel, S.; Kundu, S.; Halder, P.; Marzbali, M.H.; Chiang, K.; Surapaneni, A.; Shah, K. Production of hydrogen by catalytic methane decomposition using biochar and activated char produced from biosolids pyrolysis. *Int. J. Hydrogen Energy* **2020**, *45*, 29978–29992. [CrossRef]
173. Nishii, H.; Miyamoto, D.; Umeda, Y.; Hamaguchi, H.; Suzuki, M.; Tanimoto, T.; Harigai, T.; Takikawa, H.; Suda, Y. Catalytic activity of several carbons with different structures for methane decomposition and by-produced carbons. *Appl. Surf. Sci.* **2019**, *473*, 291–297. [CrossRef]
174. Wang, H.Y.; Lua, A.C. Hydrogen production by thermocatalytic methane decomposition. *Heat Transf. Eng.* **2013**, *34*, 896–903. [CrossRef]
175. Rahimi, N.; Gordon, M.J.; Metiu, H.; McFarland, E.W. Catalytic methane pyrolysis in molten $MnCl_2$ -KCl. *Appl. Catal. B* **2019**, *254*, 659–666.
176. Leal Pérez, B.J.; Medrano Jiménez, J.A.; Bhardwaj, R.; Goetheer, E.; van Sint Annaland, M.; Gallucci, F. Methane pyrolysis in a molten gallium bubble column reactor for sustainable hydrogen production: Proof of concept & techno-economic assessment. *Int. J. Hydrogen Energy* **2021**, *46*, 4917–4935.
177. Kang, D.; Palmer, C.; Mannini, D.; Rahimi, N.; Gordon, M.J.; Metiu, H.; McFarland, E.W. Catalytic Methane Pyrolysis in Molten Alkali Chloride Salts Containing Iron. *ACS Catal.* **2020**, *10*, 7032–7042. [CrossRef]
178. Patzschke, C.F.; Parkinson, B.; Willis, J.J.; Nandi, P.; Love, A.M.; Raman, S.; Hellgardt, K. Co-Mn catalysts for H_2 production via methane pyrolysis in molten salts. *Chem. Eng. J.* **2021**, *414*, 128730. [CrossRef]
179. Msheik, M.; Rodat, S.; Abanades, S. Methane cracking for hydrogen production: A review of catalytic and molten media pyrolysis. *Energies* **2021**, *14*, 3107. [CrossRef]
180. Parkinson, B.; Patzschke, C.F.; Nikolis, D.; Raman, S.; Dankworth, D.C.; Hellgardt, K. Methane pyrolysis in monovalent alkali halide salts: Kinetics and pyrolytic carbon properties. *Int. J. Hydrogen Energy* **2021**, *46*, 6225–6238. [CrossRef]
181. Gao, Y.; Jiang, J.; Meng, Y.; Yan, F.; Aihemaiti, A. A review of recent developments in hydrogen production via biogas dry reforming. *Energy Convers. Manag.* **2018**, *171*, 133–155. [CrossRef]
182. Ferreira-Pinto, L.; Parizi, M.P.S.; de Arau´jo, P.C.C.; Zanette, A.F.; Cardozo-Filho, L. Experimental basic factors in the production of H_2 via supercritical water gasification. *Int. J. Hydrogen Energy* **2019**, *44*, 25365–25383. [CrossRef]
183. Zhao, X.; Joseph, B.; Kuhn, J.; Ozcan, S. Biogas reforming to syngas: A review. *iScience* **2020**, *23*, 101082. [CrossRef]
184. Tsodikov, M.V.; Arapova, O.V.; Konstantinov, G.I.; Bukhtenko, O.V.; Ellert, O.G.; Nikolaev, S.A.; Vasil'kov, A.Y. The role of nanosized nickel particles in microwave-assisted dry reforming of lignin. *Chem. Eng. J.* **2017**, *309*, 628–637. [CrossRef]

185. Shu, R.; Zhou, L.; Zhu, Z.; Luo, B.; You, H.; Zhong, Z.; He, Y. Enhanced hydrogenolysis of enzymatic hydrolysis lignin over in situ prepared RuNi bimetallic catalyst. *Int. J. Hydrogen Energy* **2022**, *47*, 41564–41572. [CrossRef]
186. Weng, S.-F.; Hsieh, H.-C.; Lee, C.-S. Hydrogen production from oxidative steam reforming of ethanol on nickel-substituted pyrochlore phase catalysts. *Int. J. Hydrogen Energy* **2017**, *42*, 2849–2860. [CrossRef]
187. Lytkina, A.A.; Orekhova, N.V.; Yaroslavtsev, A.B. Catalysts for the steam reforming and electrochemical oxidation of methanol. *Inorg. Mater.* **2018**, *54*, 1315–1329. [CrossRef]
188. Pandey, B.; Prajapati, Y.K.; Sheth, P.N. Recent progress in thermochemical techniques to produce hydrogen gas from biomass: A state of the art review. *Int. J. Hydrogen Energy* **2019**, *44*, 25384–25415. [CrossRef]
189. Kumar, A.; Daw, P.; Milstein, D. Homogeneous catalysis for sustainable energy: Hydrogen and methanol economies, fuels from biomass, and related topics. *Chem. Rev.* **2022**, *122*, 385–441. [CrossRef]
190. Pipitone, G.; Zoppi, G.; Pirone, R.; Bensaid, S. A critical review on catalyst design for aqueous phase reforming. *Int. J. Hydrogen Energy* **2022**, *47*, 151–180. [CrossRef]
191. Zoppi, G.; Pipitone, G.; Pirone, R.; Bensaid, S. Aqueous phase reforming process for the valorization of wastewater streams: Application to different industrial scenarios. *Catal. Today* **2021**, *387*, 224–236. [CrossRef]
192. Therdthianwong, S.; Srisiriwat, N.; Therdthianwong, A.; Croiset, E. Reforming of bioethanol over Ni/Al_2O_3 and $Ni/CeZrO_2/Al_2O_3$ catalysts in supercritical water for hydrogen production. *Int. J. Hydrogen Energy* **2011**, *36*, 2877–2886. [CrossRef]
193. Mironova, E.Y.; Lytkina, A.A.; Ermilova, M.M.; Efimov, M.N.; Zemtsov, L.M.; Orekhova, N.V.; Karpacheva, G.P.; Bondarenko, G.N.; Yaroslavtsev, A.B.; Muraviev, D.N. Ethanol and methanol steam reforming on transition metal catalysts supported on detonation synthesis nanodiamonds for hydrogen production. *Int. J. Hydrogen Energy* **2015**, *40*, 3557–3565. [CrossRef]
194. Li, D.; Li, X.; Gong, J. Catalytic reforming of oxygenates: State of the art and future prospects. *Chem. Rev.* **2016**, *116*, 11529–11653. [CrossRef]
195. He, J.; Yang, Z.; Zhang, L.; Li, Y.; Pan, L. Cu supported on ZnAl-LDHs precursor prepared by in-situ synthesis method on γ-Al_2O_3 as catalytic material with high catalytic activity for methanol steam reforming. *Int. J. Hydrogen Energy* **2017**, *42*, 9930–9937. [CrossRef]
196. Qing, S.-J.; Hou, X.-N.; Liu, Y.-J.; Wang, L.; Li, L.-D.; Gao, Z.-X. Catalytic performance of Cu-Ni-Al spinel for methanol steam reforming to hydrogen. *J. Fuel Chem. Technol.* **2018**, *46*, 1210–1217. [CrossRef]
197. Scotti, N.; Bossola, F.; Zaccheria, F.; Ravasio, N. Copper–zirconia catalysts: Powerful multifunctional catalytic tools to approach sustainable processes. *Catalysts* **2020**, *10*, 168. [CrossRef]
198. Lytkina, A.A.; Orekhova, N.V.; Ermilova, M.M.; Petriev, I.S.; Baryshev, M.G.; Yaroslavtsev, A.B. Ru-Rh based catalysts for hydrogen production via methanol steam reforming in conventional and membrane reactors. *Int. J. Hydrogen Energy* **2019**, *44*, 13310–13322. [CrossRef]
199. Li, J.; Mei, X.; Zhang, L.; Yu, Z.; Liu, Q.; Wei, T.; Wu, W.; Dong, D.; Xu, L.; Hu, X. A comparative study of catalytic behaviors of Mn, Fe, Co, Ni, Cu and Zn-based catalysts in steam reforming of methanol, acetic acid and acetone. *Int. J. Hydrogen Energy* **2020**, *45*, 3815–3832. [CrossRef]
200. Mosinska, M.; Stępińska, N.; Maniukiewicz, W.; Rogowski, J.; Mierczynska-Vasilev, A.; Vasilev, K.; Szynkowska, M.I.; Mierczyński, P. Hydrogen production on Cu-Ni catalysts via the oxy-steam reforming of methanol. *Catalysts* **2020**, *10*, 273. [CrossRef]
201. Chen, L.; Qi, Z.; Peng, X.; Chen, J.-L.; Pao, C.-W.; Zhang, X.; Dun, C.; Young, M.; Prendergast, D.; Urban, J.J.; et al. Insights into the mechanism of methanol steam reforming tandem reaction over CeO_2 supported single-site Catalysts. *J. Am. Chem. Soc.* **2021**, *143*, 12074–12081. [CrossRef]
202. Ranjekar, A.M.; Yadav, G.D. Steam reforming of methanol for hydrogen production: A critical analysis of catalysis, processes, and scope. *Ind. Eng. Chem. Res.* **2021**, *60*, 89–113. [CrossRef]
203. Wichert, M.; Zapf, R.; Ziogas, A.; Kolb, G.; Klemm, E. Kinetic investigations of the steam reforming of methanol over a $Pt/In_2O_3/Al_2O_3$ catalyst in microchannels. *Chem. Eng. Sci.* **2016**, *155*, 201–209. [CrossRef]
204. Greluk, M.; Słowik, G.; Rotko, M.; Machocki, A. Steam reforming and oxidative steam reforming of ethanol over $PtKCo/CeO_2$ catalyst. *Fuel* **2016**, *183*, 518–530. [CrossRef]
205. Prasongthum, N.; Xiao, R.; Zhang, H.; Tsubaki, N.; Natewong, P.; Reubroycharoen, P. Highly active and stable Ni supported on CNTs-SiO_2 fiber catalysts for steam reforming of ethanol. *Fuel Process. Technol.* **2017**, *160*, 185–195. [CrossRef]
206. Mulewa, W.; Tahir, M.; Amin, N.A.S. MMT-supported Ni/TiO_2 nanocomposite for low temperature ethanol steam reforming toward hydrogen production. *Chem. Eng. J.* **2017**, *326*, 956–969. [CrossRef]
207. Montero, C.; Remiro, A.; Benito, P.L.; Bilbao, J.; Gayubo, A.G. Optimum operating conditions in ethanol steam reforming over a Ni/La_2O_3-αAl_2O_3 catalyst in a fluidized bed reactor. *Fuel Process. Technol.* **2018**, *169*, 207–216. [CrossRef]
208. Tran, S.B.T.; Choi, H.; Oh, S.; Park, J.Y. Defective Nb_2O_5-supported Pt catalysts for CO oxidation: Promoting catalytic activity via oxygen vacancy engineering. *J. Catal.* **2019**, *375*, 124–134. [CrossRef]
209. Ploner, K.; Schlicker, L.; Gili, A.; Gurlo, A.; Doran, A.; Zhang, L.; Armbrüster, M.; Obendorf, D.; Bernardi, J.; Klötzer, B.; et al. Reactive metal-support interaction in the Cu-In_2O_3 system: Intermetallic compound formation and its consequences for CO_2-selective methanol steam reforming. *Sci. Technol. Adv. Mater.* **2019**, *20*, 356–366. [CrossRef] [PubMed]
210. Lytkina, A.A.; Orekhova, N.V.; Ermilova, M.M.; Yaroslavtsev, A.B. The influence of the support composition and structure ($M_xZr_{1-x}O_{2-\delta}$) of bimetallic catalysts on the activity in methanol steam reforming. *Int. J. Hydrogen Energy* **2018**, *43*, 198–207. [CrossRef]

211. Abrokwah, R.Y.; Deshmane, V.G.; Kuila, D. Comparative performance of M-MCM-41 (M: Cu, Co, Ni, Pd, Zn and Sn) catalysts for steam reforming of methanol. *J. Molec. Catal. A* **2016**, *425*, 10–20. [CrossRef]
212. Khani, Y.; Tahay, P.; Bahadoran, F.; Safaria, N.; Soltanali, S.; Alavi, A. Synergic effect of heat and light on the catalytic reforming of methanol over Cu/x-TiO_2(x=La, Zn, Sm, Ce) nanocatalysts. *Appl. Catal. A* **2020**, *594*, 117456. [CrossRef]
213. Lytkina-Payen, A.; Tabachkova, N.; Yaroslavtsev, A. Methanol Steam Reforming on Bimetallic Catalysts Based on In and Nb Doped Titania or Zirconia: A Support Effect. *Processes* **2022**, *10*, 19. [CrossRef]
214. Kasyanova, A.V.; Rudenko, A.O.; Lyagaeva, J.G.; Medvedev, D.A. Lanthanum-containing proton-conducting electrolytes with perovskite structures. *Membr. Membr. Technol.* **2021**, *3*, 73–97. [CrossRef]
215. Zhang, J.; Su, D.S.; Blume, R.; Schlogl, R.; Wang, R.; Yang, X.; Gajovic, A. Surface Chemistry and Catalytic Reactivity of a Nanodiamond in the Steam-Free Dehydrogenation of Ethylbenzene. *Angew. Chem. Int. Ed.* **2010**, *49*, 8640–8644. [CrossRef]
216. Lytkina, A.A.; Orekhova, N.V.; Ermilova, M.M.; Belenov, S.V.; Guterman, V.E.; Efimov, M.N.; Yaroslavtsev, A.B. Bimetallic carbon nanocatalysts for methanol steam reforming in conventional and membrane reactors. *Catal. Today* **2016**, *268*, 60–67. [CrossRef]
217. Zhang, C.; Kang, X.; Liang, N.; Abdullah, A. Improvement of Biohydrogen Production from Dark Fermentation by Cocultures and Activated Carbon Immobilization. *Energy Fuels* **2017**, *31*, 12217–12222. [CrossRef]
218. Bundhoo, Z.M.A. Potential of Bio-Hydrogen Production from Dark Fermentation of Crop Residues: A Review. *Int. J. Hydrogen Energy* **2019**, *44*, 17346–17362. [CrossRef]
219. Abdin, Z.; Zafaranloo, A.; Rafiee, A.; Mérida, W.; Lipiński, W.; Khalilpour, K.R. Hydrogen as an Energy Vector. *Renew. Sustain. Energy Rev.* **2020**, *120*, 109620. [CrossRef]
220. Singh, R.; White, D.; Demirel, Y.; Kelly, R.; Noll, K.; Blum, P. Uncoupling fermentative synthesis of molecular hydrogen from biomass formation in Thermotoga maritima. *Appl. Environ. Microbiol.* **2018**, *84*, e00998-18. [CrossRef]
221. Eroglu, E.; Melis, A. Photobiological Hydrogen Production: Recent Advances and State of the Art. *Bioresour. Technol.* **2011**, *102*, 8403–8413. [CrossRef]
222. Baeyens, J.; JiapeiNie, H.; Appels, L.; Devil, R.; Ansart, R.; Deng, Y. Reviewing the potential of bio-hydrogen production by fermentation. *Renew. Sustain. Energy Rev.* **2020**, *131*, 110023. [CrossRef]
223. Hosseini, S.E.; Wahid, M.A. Hydrogen Production from Renewable and Sustainable Energy Resources: Promising Green Energy Carrier for Clean Development. *Renew. Sustain. Energy Rev.* **2016**, *57*, 850–866. [CrossRef]
224. Sha-habuddin, M.; Krishna, B.B.; Bhaskar, T.; Perkins, G. Advances in the Thermo-Chemical Production of Hydrogen from Biomass and Residual Wastes: Summary of Recent Techno-Economic Analyzes. *Bioresour. Technol.* **2020**, *299*, 122557. [CrossRef]
225. Makaryan, I.A.; Sedov, I.V.; Maksimov, A.L. Hydrogen storage using liquid organic carriers. *Russ. J. Appl. Chem.* **2020**, *93*, 1815–1830. [CrossRef]
226. Rivard, E.; Trudeau, M.; Zaghi, K. Hydrogen storage for mobility: A review. *Materials* **2019**, *12*, 1973. [CrossRef] [PubMed]
227. Xu, X.; Liu, E.; Zhu, N.; Liu, F.; Qian, F. Review of the current status of ammonia-blended hydrogen fuel engine development. *Energies* **2022**, *15*, 1023. [CrossRef]
228. Wang, P.; Chang, F.; Gao, W.; Guo, J.; Wu, G.; He, T.; Chen, P. Breaking scaling relations to achieve low-temperature ammonia synthesis through LiH-mediated nitrogen transfer and hydrogenation. *Nat. Chem.* **2016**, *9*, 64–70. [CrossRef] [PubMed]
229. Aika, K.-I. Role of alkali promoter in ammonia synthesis over ruthenium catalysts—Effect on reaction mechanism. *Catal. Today* **2017**, *286*, 14–20. [CrossRef]
230. Mironova, E.Y.; Ermilova, M.M.; Orekhova, N.V.; Tolkacheva, A.S.; Shkerin, S.N.; Yaroslavtsev, A.B. Transformations of ethanol on catalysts based on nanoporous calcium aluminate, mayenite ($Ca_{12}Al_{14}O_{33}$),and mayenite doped by copper. *Nanotechnol. Russia* **2017**, *12*, 597–604. [CrossRef]
231. Flimban, S.G.A.; Hassan, S.H.A.; Rahman, M.M.; Oh, S.-E. The effect of Nafion membrane fouling on the power generation of a microbial fuel cell. *Int. J. Hydrogen Energy* **2020**, *45*, 13643–13651. [CrossRef]
232. Jeerh, G.; Zhang, M.; Tao, S. Recent progress in ammonia fuel cells and their potential applications. *J. Mater. Chem. A* **2021**, *9*, 727–752. [CrossRef]
233. Geburtig, D.; Preuster, P.; Boesmann, A.; Mueller, K.; Wasserscheid, P. Chemical utilization of hydrogen from fluctuating energy sources—Catalytic transfer hydrogenation from charged Liquid Organic Hydrogen Carrier systems. *Int. J. Hydrogen Energy* **2016**, *41*, 1010–1017. [CrossRef]
234. Makepeace, J.W.; He, T.; Weidenthaler, C.; Jensen, T.R.; Chang, F.; Vegge, T.; Ngene, P.; Kojima, Y.; de Jongh, P.E.; Chen, P.; et al. Reversible ammonia-based and liquid organic hydrogen carriers for high-density hydrogen storage: Recent progress. *Int. J. Hydrogen Energy* **2019**, *44*, 7746–7767. [CrossRef]
235. Kustov, L.M.; Kalenchuk, A.N.; Bogdan, V.I. Systems for accumulation, storage and release of hydrogen. *Russ. Chem. Rev.* **2020**, *89*, 897–916. [CrossRef]
236. Wijayanta, A.T.; Oda, T.; Purnomo, C.W.; Kashiwagi, T.; Aziz, M. Liquid hydrogen, methylcyclohexane, and ammonia as potential hydrogen storage: Comparison review. *Int. J. Hydrogen Energy* **2019**, *44*, 15026–15044. [CrossRef]
237. Dong, Y.; Yang, M.; Li, L.; Zhu, T.; Chen, X.; Cheng, H. Study on reversible hydrogen uptake and release of 1,2-dimethylindole as a new liquid organic hydrogen carrier. *Int. J. Hydrogen Energy* **2019**, *44*, 4919–4929. [CrossRef]
238. Tan, K.C.; He, T.; Chua, Y.S.; Chen, P. Recent Advances of Catalysis in the Hydrogenation and Dehydrogenation of N-Heterocycles for Hydrogen Storage. *J. Phys. Chem. C* **2021**, *125*, 18553–18566. [CrossRef]

239. Kim, Y.; Song, Y.; Choi, Y.; Jeong, K.; Park, J.H.; Ko, K.C.; Na, K. Catalytic Consequences of Supported Pd Catalysts on Dehydrogenative H_2 Evolution from 2-[(n-Methylcyclohexyl)methyl]piperidine as the Liquid Organic Hydrogen Carrier. *ACS Sustain. Chem. Eng.* **2021**, *9*, 809–821. [CrossRef]
240. Liu, H.; Zhou, C.; Li, W.; Li, W.; Qiu, M.; Chen, X.; Wang, H.; Sun, Y. Ultralow Rh Bimetallic Catalysts with High Catalytic Activity for the Hydrogenation of N-Ethylcarbazole. *ACS Sustain. Chem. Eng.* **2021**, *9*, 5260–5267. [CrossRef]
241. Mollar-Cuni, A.; Ventura-Espinosa, D.; Martín, S.; García, H.; Mata, J.A. Reduced Graphene Oxides as Carbocatalysts in Acceptorless Dehydrogenation of N-Heterocycles. *ACS Catal.* **2021**, *11*, 14688–14693. [CrossRef]
242. Mejuto, C.; Ibáñez-Ibáñez, L.; Guisado-Barrios, G.; Mata, J.A. Visible-Light-Promoted Iridium(III)-Catalyzed Acceptorless Dehydrogenation of N-Heterocycles at Room Temperature. *ACS Catal.* **2022**, *12*, 6238–6245. [CrossRef]
243. Lim, S.; Song, Y.; Jeong, K.; Park, J.H.; Na, K. Enhanced Dehydrogenative H_2 Release from N-Containing Amphicyclic LOHC Boosted by Pd-Supported Nanosheet MFI Zeolites Having Strong Acidity and Large Mesoporosity. *ACS Sustain. Chem. Eng.* **2022**, *10*, 3584–3594. [CrossRef]
244. Li, L.; Yang, M.; Dong, Y.; Mei, P.; Cheng, H. Hydrogen storage and release from a new promising Liquid Organic Hydrogen Storage Carrier (LOHC): 2-methylindole. *Int. J. Hydrogen Energy* **2016**, *41*, 16129–16134. [CrossRef]
245. Muller, K.; Stark, K.; Mueller, B.; Arlt, W. Amine Borane Based Hydrogen Carriers: An Evaluation. *Energy Fuel* **2012**, *26*, 3691–3696. [CrossRef]
246. Preuster, P.; Papp, C.; Wasserscheid, P. Liquid organic hydrogen carriers (LOHCs): Toward a hydrogen-free hydrogen economy. *Acc. Chem. Res.* **2017**, *50*, 74–85. [CrossRef]
247. Nafchi, F.M.; Baniasadi, E.; Afshari, E.; Javani, N. Performance assessment of a solar hydrogen and electricity production plant using high temperature PEM electrolyzer and energy storage. *Int. J. Hydrogen Energy* **2018**, *43*, 5820–5831. [CrossRef]
248. Auer, F.; Blaumeiser, D.; Bauer, T.; Bösmann, A.; Szesni, N.; Libuda, J.; Wasserscheid, P. Boosting the activity of hydrogen release from liquid organic hydrogen carrier systems by sulfur-additives to Pt on alumina catalysts. *Catal. Sci. Technol.* **2019**, *9*, 3537–3547. [CrossRef]
249. Wang, W.; Miao, L.; Wu, K.; Chen, G.; Huang, Y.; Yang, Y. Hydrogen evolution in the dehydrogenation of methylcyclohexane over Pt/CeMgAlO catalysts derived from their layered double hydroxides. *Int. J. Hydrogen Energy* **2019**, *44*, 2918–2925. [CrossRef]
250. Zhu, T.; Yang, M.; Chen, X.; Dong, Y.; Zhang, Z.; Cheng, H. A highly active bifunctional Ru–Pd catalyst for hydrogenation and dehydrogenation of liquid organic hydrogen carriers. *J. Catal.* **2019**, *378*, 382–391. [CrossRef]
251. Aakko-Saksa, P.T.; Vehkamaki, M.; Kemell, M.; Keskivali, L.; Simell, P.; Reinikainen, M.; Tapper, U.; Repo, T. Hydrogen release from liquid organic hydrogen carriers catalysed by platinum on rutileanatase structured titania. *Chem. Commun.* **2020**, *56*, 1657–1660. [CrossRef] [PubMed]
252. Shi, L.; Zhou, Y.; Qi, S.; Smith, K.J.; Tan, X.; Yan, J.; Yi, C. Pt Catalysts Supported on H_2 and O_2 Plasma-Treated Al_2O_3 for Hydrogenation and Dehydrogenation of the Liquid Organic Hydrogen Carrier Pair Dibenzyltoluene and Perhydrodibenzyltoluene. *ACS Catal.* **2020**, *10*, 10661–10671. [CrossRef]
253. Hamayun, M.H.; Maafa, I.M.; Hussain, M.; Aslam, R. Simulation study to investigate the efects of operational conditions on methylcyclohexane dehydrogenation for hydrogen production. *Energies* **2020**, *13*, 206. [CrossRef]
254. Chen, X.; Gierlich, C.H.; Schötz, S.; Blaumeiser, D.; Bauer, T.; Libuda, J.; Palkovits, R. Hydrogen Production Based on Liquid Organic Hydrogen Carriers through Sulfur Doped Platinum Catalysts Supported on TiO_2. *ACS Sustain. Chem. Eng.* **2021**, *9*, 6561–6573. [CrossRef]
255. Bellows, S.M.; Chakraborty, S.; Gary, J.B.; Jones, W.D.; Cundari, T.R. An uncanny dehydrogenation mechanism: Polar bond control over stepwise or concerted transition states. *Inorg. Chem.* **2017**, *56*, 5519–5524. [CrossRef]
256. Bernskoetter, W.H.; Hazari, N. Hydrogenation and dehydrogenation reactions catalyzed by iron pincer compounds. In *Pincer Compounds*, 1st ed.; Morales-Morales, D., Ed.; Elsevier: Amsterdam, The Netherlands, 2018; pp. 111–131.
257. Sisáková, K.; Podrojková, N.; Oriňaková, R.; Oriňak, A. Novel catalysts for dibenzyltoluene as a potential Liquid Organic Hydrogen Carrier use—A mini-review. *Energy Fuels* **2021**, *35*, 7608–7623. [CrossRef]
258. Stenina, I.A.; Safronova, E.Y.; Levchenko, A.V.; Dobrovolsky, Y.A.; Yaroslavtsev, A.B. Low-temperature fuel cells: Outlook for application in energy storage systems and materials for their development. *Therm. Eng.* **2016**, *63*, 385–398. [CrossRef]
259. Jeppesen, C.; Polverino, P.; Andreasen, S.J.; Araya, S.S.; Sahlin, S.L.; Pianese, C.; Kær, S.K. Impedance characterization of high temperature proton exchange membrane fuel cell stack under the influence of carbon monoxide and methanol vapor. *Int. J. Hydrogen Energy* **2017**, *42*, 21901–21912. [CrossRef]
260. Sutharssan, T.; Montalvao, D.; Chen, Y.K.; Wang, W.C.; Pisac, C.; Elemara, H. A review on prognostics and health monitoring of proton exchange membrane fuel cell. *Renew. Sustain. Energy Rev.* **2017**, *75*, 440–450. [CrossRef]
261. Briceño, K.; Montanè, D.; Garcia-Valls, R.; Iulianelli, A.; Basile, A. Fabrication variables affecting the structure and properties of supported carbon molecular sieve membranes for hydrogen separation. *J. Membr. Sci.* **2012**, *415*, 288–297. [CrossRef]
262. Sazali, N.; Mohamed, M.A.; Salleh, W.N.W. Membranes for hydrogen separation: A significant review. *Int. J. Adv. Manuf. Technol.* **2020**, *107*, 1859–1881. [CrossRef]
263. Rezaee, P.; Naeij, H.R. A new approach to separate hydrogen from carbon dioxide using graphdiyne-like membrane. *Sci. Rep.* **2020**, *10*, 13549. [CrossRef]
264. Cheng, H. Dual-Phase Mixed Protonic-Electronic Conducting Hydrogen Separation Membranes: A Review. *Membranes* **2022**, *12*, 647. [CrossRef]

265. Arratibel, A.; Astobieta, U.; Pacheco Tanaka, D.A.; van Sint Annaland, M.; Gallucci, F. N_2, He and CO_2 diffusion mechanism through nanoporous YSZ/γ-Al_2O_3 layers and their use in a pore-filled membrane for hydrogen membrane reactors. *Int. J. Hydrogen Energy* **2016**, *41*, 8732–8744. [CrossRef]
266. Kim, C.-H.; Han, J.-Y.; Kim, S.; Lee, B.; Lim, H.; Lee, K.-Y.; Ryi, S.-K. Hydrogen production by steam methane reforming in a membrane reactor equipped with a Pd composite membrane deposited on a porous stainless steel. *Int. J. Hydrogen Energy* **2018**, *43*, 7684–7692. [CrossRef]
267. Fernandez, E.; Helmi, A.; Medrano, J.; Coenen, K.; Arratibel, A.; Melendez, J.; de Nooijer, N.; Spallina, V.; Viviente, J.L.; Zuniga, J. Palladium based membranes and membrane reactors for hydrogen production and purification: An overview of research activities at Tecnalia and Tu/e. *Int. J. Hydrogen Energy* **2017**, *42*, 13763–13776. [CrossRef]
268. Fernandez, E.; Medrano, J.A.; Melendez, J.; Parco, M.; Viviente, J.L.; Van Sint Annaland, M.; Gallucci, F.; Tanaka, P.D.A. Preparation and characterization of metallic supported thin Pd–Ag membranes for hydrogen separation. *Chem. Eng. J.* **2016**, *305*, 182–190. [CrossRef]
269. Pati, S.; Jat, R.A.; Mukerjee, S.; Parida, S. X-ray diffraction study of thermal parameters of Pd, Pd–Ag and Pd–Ag–Cu alloys as hydrogen purification membrane materials. *Physica B Cond. Matter* **2016**, *484*, 42–47. [CrossRef]
270. Sharma, R.; Kumar, A.; Upadhyay, R.K. Performance comparison of methanol steam reforming integrated to Pd-Ag membrane: Membrane reformer vs. membrane separator. *Sep. Purif. Technol.* **2017**, *183*, 194–203. [CrossRef]
271. Zhao, C.; Sun, B.; Jiang, J.; Xu, W. H_2 purification process with double layer bcc-PdCu alloy membrane at ambient temperature. *Int. J. Hydrogen Energy* **2020**, *45*, 17540–17547. [CrossRef]
272. Ievlev, V.M.; Prizhimov, A.S.; Dontsov, A.I. Structure of the α–β Interface in a PdCu Solid Solution. *Phys. Solid State* **2020**, *62*, 59–64. [CrossRef]
273. El Hawa, H.A.W.; Paglieri, S.; Craig, M.C.; Harale, A.; Way, D.J. Application of a Pd–Ru composite membrane to hydrogen production in a high temperature membrane reactor. *Sep. Purif. Technol.* **2015**, *147*, 388–397. [CrossRef]
274. Lee, S.M.; Xu, N.; Kim, S.S.; Li, A.; Grace, J.R.; Lim, J.C.; Boyd, T.; Ryi, S.K.; Susdorf, A.; Schaadt, A. Palladium/ruthenium composite membrane for hydrogen separation from the off-gas of solar cell production via chemical vapor deposition. *J. Membr. Sci.* **2017**, *541*, 1–8. [CrossRef]
275. Ievlev, V.M.; Maksimenko, A.A.; Sitnikov, A.I.; Solntsev, K.A.; Chernyavskiy, A.S.; Dontsov, A.I. Composite metal-ceramic heterostructure for membranes of deep purification of hydrogen. *Inorg. Mater. Appl. Res.* **2016**, *7*, 586–589. [CrossRef]
276. Plazaola, A.; Tanaka, D.A.P.; Van Sint Annaland, M.; Gallucci, F. Recent Advances in Pd-Based Membranes for Membrane Reactors. *Molecules* **2017**, *22*, 51. [CrossRef]
277. Alimov, V.N.; Bobylev, I.V.; Busnyuk, A.O.; Kolgatin, S.N.; Kuzenov, S.R.; Peredistov, E.Y.; Livshits, A.I. Extraction of ultrapure hydrogen with V-alloy membranes: From laboratory studies to practical applications. *Int. J. Hydrogen Energy* **2018**, *43*, 13318–13327. [CrossRef]
278. Helmi, A.; Fernandez, E.; Melendez, J.; Tanaka, D.A.P.; Gallucci, F.; van Sint Annaland, M. Fluidized Bed Membrane Reactors for Ultra Pure H_2 Production—A Step forward towards Commercialization. *Molecules* **2016**, *21*, 376. [CrossRef] [PubMed]
279. Iulianelli, A.; Ghasemzadeh, K.; Basile, A. Progress in Methanol Steam Reforming Modelling via Membrane Reactors Technology. *Membranes* **2018**, *8*, 65. [CrossRef] [PubMed]
280. Franchi, G.; Capocelli, M.; De Falco, M.; Piemonte, V.; Barba, D. Hydrogen Production via Steam Reforming: A Critical Analysis of MR and RMM Technologies. *Membranes* **2020**, *10*, 10. [CrossRef]
281. Liguori, S.; Iulianelli, A.; Dalena, F.; Piemonte, V.; Huang, Y.; Basile, A. Methanol steam reforming in an Al_2O_3 supported thin pd-layer membrane reactor over Cu/ZnO/Al_2O_3 catalyst. *Int. J. Hydrogen Energy* **2014**, *39*, 18702–18710. [CrossRef]
282. Piskin, F.; Öztürk, T. Combinatorial screening of Pd-Ag-Ni membranes for hydrogen separation. *J. Memb. Sci.* **2017**, *524*, 631–636. [CrossRef]
283. Mironova, E.Y.; Dontsov, A.I.; Morozova, N.B.; Gorbunov, S.V.; Ievlev, V.M.; Yaroslavtsev, A.B. Lamp Processing of the Surface of PdCu Membrane Foil: Hydrogen Permeability and Membrane Catalysis. *Inorg. Mater.* **2021**, *57*, 781–789. [CrossRef]
284. Fernandez, E.; Sanchez-Garcia, J.A.; Melendez, J.; Spallina, V.; van Sint Annaland, M.; Gallucci, F.; Tanaka, D.P.; Prema, R. Development of highly permeable ultra-thin Pd-based supported membranes. *Chem. Eng. J.* **2016**, *305*, 149–155. [CrossRef]
285. Pati, S.; Jat, R.A.; Anand, N.; Derose, D.J.; Karn, K.; Mukerjee, S.; Parida, S. Pd-Ag-Cu dense metallic membrane for hydrogen isotope purification and recovery at low pressures. *J. Memb. Sci.* **2017**, *522*, 151–158. [CrossRef]
286. Incelli, M.; Santucci, A.; Tosti, S.; Sansovini, M.; Carlini, M. Heavy water decontamination tests through a pd-ag membrane reactor: Water gas shift and isotopic swamping performances. *Fusion Eng. Des.* **2017**, *124*, 692–695. [CrossRef]
287. Pati, S.; Jangam, A.; Wang, Z.; Dewangan, N.; Wai, M.H.; Kawi, S. Catalytic $Pd_{0.77}Ag_{0.23}$ alloy membrane reactor for high temperature water-gas shift reaction: Methane suppression. *Chem. Eng. J.* **2019**, *362*, 116–125. [CrossRef]
288. Kurokawa, H.; Yakabe, H.; Yasuda, I.; Peters, T.; Bredesen, R. Inhibition effect of CO on hydrogen permeability of Pd–Ag membrane applied in a microchannel module configuration. *Int. J. Hydrogen Energy* **2014**, *39*, 17201–17209. [CrossRef]
289. Gallucci, F.; Basile, A.; Tosti, S.; Iulianelli, A.; Drioli, E. Membrane catalysis in the dehydrogenation and hydrogen production processes. *Int. J. Hydrogen Energy* **2007**, *32*, 1201. [CrossRef]
290. Ghasemzadeh, K.; Harasi, J.; Amiri, T.; Basile, A.; Iulianelli, A. Methanol steam reforming for hydrogen generation: A comparative modeling study between silica and Pd-based membrane reactors by cfd method. *Fuel Process. Technol.* **2020**, *199*, 106273. [CrossRef]

291. Borgognoni, F.; Tosti, S.; Vadrucci, M.; Santucci, A. Combined methane and ethanol reforming for pure hydrogen production through pd-based membranes. *Int. J. Hydrogen Energy* **2013**, *38*, 1430–1438. [CrossRef]
292. Jia, H.; Zhang, J.; Yu, J.; Yang, X.; Sheng, X.; Xu, H.; Sun, C.; Shen, W.; Goldbach, A. Efficient H_2 production via membrane-assisted ethanol steam reforming over Ir/CeO_2 catalyst. *Int. J. Hydrogen Energy* **2019**, *44*, 24733–24745. [CrossRef]
293. Lytkina, A.A.; Mironova, E.Y.; Orekhova, N.V.; Ermilova, M.M.; Yaroslavtsev, A.B. Ru-containing catalysts for methanol and ethanol steam reforming in conventional and membrane reactors. *Inorg. Mater.* **2019**, *55*, 547–555. [CrossRef]
294. Jia, H.; Xu, H.; Sheng, X.; Yang, X.; Shen, W.; Goldbach, A. Hightemperature ethanol steam reforming in PdCu membrane reactor. *J. Memb. Sci.* **2020**, *605*, 118083. [CrossRef]
295. Li, C.; He, Z.; Ban, X.; Li, N.; Chen, C.; Zhan, Z. Membrane-based catalytic partial oxidation of ethanol coupled with steam reforming for solid oxide fuel cells. *J. Membr. Sci.* **2021**, *622*, 119032. [CrossRef]
296. Eremeev, N.; Krasnov, A.; Bespalko, Y.; Bobrova, L.; Smorygo, O.; Sadykov, V. An Experimental Performance Study of a Catalytic Membrane Reactor for Ethanol Steam Reforming over a Metal Honeycomb Catalyst. *Membranes* **2021**, *11*, 790. [CrossRef]
297. Viviente, J.L.; Meléndez, J.; Tanaka, D.A.P.; Gallucci, F.; Spallina, V.; Manzolini, G.; Foresti, S.; Palma, V.; Ruocco, C.; Roses, L. Advanced m-chp fuel cell system based on a novel bio-ethanol fluidized bed membrane reformer. *Int. J. Hydrogen Energy* **2017**, *42*, 13970–13987. [CrossRef]
298. Iulianelli, A.; Palma, V.; Bagnato, G.; Ruocco, C.; Huang, Y.; Veziroğlu, N.T.; Basile, A. From bioethanol exploitation to high grade hydrogen generation: Steam reforming promoted by a co-pt catalyst in a pd-based membrane reactor. *Renew. Energy* **2018**, *119*, 834–843. [CrossRef]
299. Iulianelli, A.; Longo, T.; Basile, A. CO-free hydrogen production by steam reforming of acetic acid carried out in a pd–ag membrane reactor: The effect of co-current and counter-current mode. *Int. J. Hydrogen Energy* **2008**, *33*, 4091–4096. [CrossRef]
300. Shiva Kumar, S.; Himabindu, V. Hydrogen Production by PEM Water Electrolysis—A Review. *Mater. Sci. Energy Technol.* **2019**, *2*, 442–454. [CrossRef]
301. El-Shafie, M.; Kambara, S.; Hayakawa, Y. Hydrogen production tchnologies overview. *J. Power Energy Eng.* **2019**, *7*, 107–154. [CrossRef]
302. Kayfeci, M.; Kecebas, A.; Bayat, M. Hydrogen production. In *Solar Hydrogen Production: Processes, Systems and Technologies*, 1st ed.; Calise, F., D'Accadia, M.D., Santarelli, M., Lanzini, A., Ferrero, D., Eds.; Academic Press: London, UK, 2019; pp. 45–83.
303. Skúlason, E.; Karlberg, G.S.; Rossmeisl, J.; Bligaard, T.; Greeley, J.; Jónsson, H.; Nørskov, J.K. Density functional theory calculations for the hydrogen evolution reaction in an electrochemical double layer on the Pt(111) electrode. *Phys. Chem. Chem. Phys.* **2007**, *9*, 3241–3250. [CrossRef]
304. Markovića, N.M.; Sarraf, S.T.; Gasteiger, H.A.; Ross, P.N. Hydrogen electrochemistry on platinum low-index single-crystal surfaces in alkaline solution. *J. Chem. Soc. Faraday Trans.* **1996**, *92*, 3719–3725. [CrossRef]
305. Suen, N.-T.; Hung, S.-F.; Quan, Q.; Zhang, N.; Xu, Y.-J.; Chen, H.M. Electrocatalysis for the oxygen evolution reaction: Recent development and future perspectives. *Chem. Soc. Rev.* **2017**, *46*, 337–365. [CrossRef]
306. Cook, T.R.; Dogutan, D.K.; Reece, S.Y.; Surendranath, Y.; Teets, T.S.; Nocera, D.G. Solar Energy Supply and Storage for the Legacy and Nonlegacy Worlds. *Chem. Rev.* **2010**, *110*, 6474–6502. [CrossRef]
307. Liu, L.; Wang, Y.; Zhao, Y.; Wang, Y.; Zhang, Z.; Wu, T.; Qin, W.; Liu, S.; Jia, B.; Wu, H.; et al. Ultrahigh Pt-Mass-Activity Hydrogen Evolution Catalyst Electrodeposited from Bulk Pt. *Adv. Funct. Mater.* **2022**, *32*, 2112207. [CrossRef]
308. Cavaliere, P.D.; Perrone, A.; Silvello, A. Water Electrolysis for the Production of Hydrogen to Be Employed in the Ironmaking and Steelmaking Industry. *Metals* **2021**, *11*, 1816. [CrossRef]
309. Stenina, I.A.; Yaroslavtsev, A.B. Nanomaterials for lithium-ion batteries and hydrogen energy. *Pure Appl. Chem.* **2017**, *89*, 1185–1194. [CrossRef]
310. Immerz, C.; Paidar, M.; Papakonstantinou, G.; Bensmann, B.; Bystron, T.; Vidakovic-Koch, T.; Bouzek, K.; Sundmacher, K.; Hanke-Rauschenbach, R. Effect of the MEA design on the performance of PEMWE single cells with different sizes. *J. Appl. Electrochem.* **2018**, *48*, 701–711. [CrossRef]
311. Giancola, S.; Zatoń, M.; Reyes-Carmona, Á.; Dupont, M.; Donnadio, A.; Cavaliere, S.; Rozière, J.; Jones, D.J. Composite short side chain PFSA membranes for PEM water electrolysis. *J. Memb. Sci.* **2019**, *570–571*, 69–76. [CrossRef]
312. Hu, C.; Zhang, L.; Gong, J. Recent progress made in the mechanism comprehension and design of electrocatalysts for alkaline water splitting. *Energy Environ. Sci.* **2019**, *12*, 2620–2645. [CrossRef]
313. Shiva Kumar, S.; Ramakrishna, S.U.B.; Srinivasulu Reddy, D.; Bhagawan, D.; Himabindu, V. Synthesis of Polysulfone and zirconium oxide coated asbestos composite separators for alkaline water electrolysis. *Int. J. Chem. Eng. Process Technol.* **2017**, *3*, 1035–1041.
314. Du, N.; Roy, C.; Peach, R.; Turnbull, M.; Thiele, S.; Bock, C. Anion-Exchange Membrane Water Electrolyzers. *Chem. Rev.* **2022**, *122*, 11830–11895. [CrossRef]
315. Laguna-Bercero, M.A. Recent advances in high temperature electrolysis using solid oxide fuel cells: A review. *J. Power Source* **2012**, *203*, 4–16. [CrossRef]
316. Nechache, A.; Hody, S. Alternative and innovative solid oxide electrolysis cell materials: A short review. *Renew. Sustain. Energy Rev.* **2021**, *149*, 111322. [CrossRef]
317. Song, Y.; Zhang, X.; Xie, K.; Wang, G.; Bao, X. High-Temperature CO_2 Electrolysis in Solid Oxide Electrolysis Cells: Developments, Challenges, and Prospects. *Adv. Mater.* **2019**, *31*, 1902033. [CrossRef]

318. Kadier, A.; Sahaid Kalil, M.; Abdeshahian, P.; Chandrasekhar, K.; Mohamed, A.; Farhana Azman, N.; Logroño, W.; Simayi, Y.; Abdul Hamid, A. Recent advances and emerging challenges in microbial electrolysis cells (MECs) for microbial production of hydrogen and value-added chemicals. *Renew. Sustain. Energy Rev.* **2016**, *61*, 501–525. [CrossRef]
319. Dotan, H.; Landman, A.; Sheehan, S.W.; Malviya, K.D.; Shter, G.E.; Grave, D.A.; Arzi, Z.; Yehudai, N.; Halabi, M.; Gal, N.; et al. Decoupled hydrogen and oxygen evolution by a two-step electrochemical–chemical cycle for efficient overall water splitting. *Nat. Energy* **2019**, *4*, 786–795. [CrossRef]
320. Shiva Kumar, S.; Ramakrishna, S.U.B.; Rama Devi, B.; Himabindu, V. Phosphorus doped carbon nanoparticles supported palladium electrocatalyst for the hydrogen evolution reaction (HER) in PEM water electrolysis. *Ionics* **2018**, *24*, 3113–3121. [CrossRef]
321. Sarkar, S.; Peter, S.C. An overview on Pd Based Electrocatalysts for Hydrogen Evolution Reaction. *Inorg. Chem. Front.* **2018**, *5*, 2060–2080. [CrossRef]
322. Martin, S.; Garcia-Ybarra, P.; Castillo, J. Ten-fold reduction from the state-of-the-art platinum loading of electrodes prepared by electrospraying for high temperature proton exchange membrane fuel cells. *Electrochem. Commun.* **2018**, *93*, 57–61. [CrossRef]
323. Lee, B.-S.; Park, H.-Y.; Choi, I.; Cho, M.K.; Kim, H.-J.; Yoo, S.J.; Henkensmeier, D.; Kim, J.Y.; Nam, S.W.; Park, S.; et al. Polarization characteristics of a low catalyst loading PEM water electrolyzer operating at elevated temperature. *J. Power Source* **2016**, *309*, 127–134. [CrossRef]
324. Ramakrishna, S.U.B.; Srinivasulu Reddy, D.; Shiva Kumar, S.; Himabindu, V. Nitrogen doped CNTs supported Palladium electrocatalyst for hydrogen evolution reaction in PEM water electrolyser. *Int. J. Hydrogen Energy* **2016**, *41*, 20447–20454. [CrossRef]
325. Li, T.-J.; Yeh, M.-H.; Chiang, W.-H.; Li, Y.-S.; Chen, G.-L.; Leu, Y.-A.; Tien, T.-C.; Lo, S.-C.; Lin, L.-Y.; Lin, J.-J.; et al. Boron-doped carbon nanotubes as metal-free electrocatalyst for dyesensitized solar cells: Heteroatom doping level effect on tri-iodide reduction reaction. *J. Power Source* **2018**, *375*, 29–36.
326. Xie, L.; Liu, Q.; Shi, X.; Asiri, A.M.; Luo, Y.; Sun, X. Superior alkaline hydrogen evolution electrocatalysis enabled by an ultrafine PtNi nanoparticle-decorated Ni nanoarray with ultralow Pt loading. *Inorg. Chem. Front.* **2018**, *5*, 1365–1369. [CrossRef]
327. Zhao, Z.; Liu, H.; Gao, W.; Xue, W.; Liu, Z.; Huang, J.; Pan, X.; Huang, Y. Surface-Engineered PtNi-O Nanostructure with Record-High Performance for Electrocatalytic Hydrogen Evolution Reaction. *J. Am. Chem. Soc.* **2018**, *140*, 9046–9050. [CrossRef]
328. Wang, Z.; Ren, X.; Luo, Y.; Wang, L.; Cui, G.; Xie, F.; Wang, H.; Xie, Y.; Sun, X. An ultrafine platinum–cobalt alloy decorated cobalt nanowire array with superb activity toward alkaline hydrogen evolution. *Nanoscale* **2018**, *10*, 12302–12307. [CrossRef] [PubMed]
329. Huang, X.-Y.; Wang, A.J.; Zhang, L.; Fang, K.-M.; Wu, L.-J.; Feng, J.J. Melamine-assisted solvothermal synthesis of PtNi nanodentrites as highly efficient and durable electrocatalyst for hydrogen evolution reaction. *J. Colloid Interface Sci.* **2018**, *531*, 578–584. [CrossRef] [PubMed]
330. Xie, Y.; Cai, J.; Wu, Y.; Zang, Y.; Zheng, X.; Ye, J.; Cui, P.; Niu, S.; Liu, Y.; Zhu, J. Boosting Water Dissociation Kinetics on Pt–Ni Nanowires by N-Induced Orbital Tuning. *Adv. Mater.* **2019**, *31*, 1807780. [CrossRef] [PubMed]
331. Wang, S.; Lu, A.; Zhong, C.-J. Hydrogen production from water electrolysis: Role of catalysts. *Nano Converg.* **2021**, *8*, 4. [CrossRef] [PubMed]
332. Levy, R.; Boudart, M. Platinum-like behavior of tungsten carbide in surface catalysis. *Science* **1973**, *181*, 547–549. [CrossRef]
333. Jimenez-Orozco, C.; Florez, E.; Moreno, A.; Rodriguez, J.A. Platinum vs transition metal carbide surfaces as catalysts for olefin and alkyne conversion: Binding and hydrogenation of ethylidyne. *J. Phys. Conf. Ser.* **2019**, *1247*, 012003. [CrossRef]
334. Vrubel, H.; Hu, X. Molybdenum Boride and Carbide Catalyze Hydrogen Evolution in both Acidic and Basic Solutions. *Angew. Chem. Int. Ed.* **2012**, *51*, 12703–12706. [CrossRef]
335. Gao, W.; Shi, Y.; Zhang, Y.; Zuo, L.; Lu, H.; Huang, Y.; Fan, W.; Liu, T. Molybdenum carbide anchored on graphene nanoribbons as highly efficient all-pH hydrogen evolution reaction electrocatalyst. *ACS Sustain. Chem. Eng.* **2016**, *4*, 6313–6321. [CrossRef]
336. Zhang, R.; Wang, X.; Yu, S.; Wen, T.; Zhu, X.; Yang, F.; Sun, X.; Wang, X.; Hu, W. Ternary $NiCo_2P_x$ Nanowires as pH-Universal Electrocatalysts for Highly Efficient Hydrogen Evolution Reaction. *Adv. Mater.* **2017**, *29*, 1605502. [CrossRef]
337. Wang, H.; Xiao, X.; Liu, S.; Chiang, C.-L.; Kuai, X.; Peng, C.-K.; Lin, Y.-C.; Meng, X.; Zhao, J.; Choi, J.; et al. Structural and Electronic Optimization of MoS_2 Edges for Hydrogen Evolution. *J. Am. Chem. Soc.* **2019**, *141*, 18578–18584. [CrossRef]
338. Han, D.; Gao, N.; Ge, J.; Liu, C.; Xing, W. Activating MoS_2 via electronic structure modulation and phase engineering for hydrogen evolution reaction. *Catal. Commun.* **2022**, *164*, 106427. [CrossRef]
339. Sarno, M.; Ponticorvo, E. High hydrogen production rate on RuS_2@MoS_2 hybrid nanocatalyst by PEM electrolysis. *Int. J. Hydrogen Energy* **2019**, *44*, 4398–4405. [CrossRef]
340. Grimaud, A.; Diaz-Morales, O.; Han, B.; Hong, W.T.; Lee, Y.-L.; Giordano, L.; Stoerzinger, K.A.; Koper, M.T.; Shao-Horn, Y. Activating lattice oxygen redox reactions in metal oxides to catalyse oxygen evolution. *Nat. Chem.* **2017**, *9*, 457–465. [CrossRef]
341. Huang, Z.F.; Song, J.; Du, Y.; Xi, S.; Dou, S.; Nsanzimana, J.M.V.; Wang, C.; Xu, Z.J.; Wang, X. Chemical and structural origin of lattice oxygen oxidation in Co–Zn oxyhydroxide oxygen evolution electrocatalysts. *Nat. Energy* **2019**, *4*, 329–338. [CrossRef]
342. Zhu, Y.; Tahini, H.A.; Hu, Z.; Chen, Z.G.; Zhou, W.; Komarek, A.C.; Lin, Q.; Lin, H.J.; Chen, C.T.; Zhong, Y.; et al. Boosting Oxygen Evolution Reaction by Creating Both Metal Ion and Lattice-Oxygen Active Sites in a Complex Oxide. *Adv. Mater.* **2020**, *32*, 1905025. [CrossRef]
343. Shan, S.; Li, J.; Maswadeh, Y.; O'Brien, C.; Kareem, H.; Tran, D.T.; Lee, I.C.; Wu, Z.P.; Wang, S.; Yan, S.; et al. Surface Oxygenation of Multicomponent Nanoparticles toward Active and Stable Oxidation Catalysts. *Nat. Commun.* **2020**, *11*, 4201. [CrossRef]

344. Mefford, J.T.; Rong, X.; Abakumov, A.M.; Hardin, W.G.; Dai, S.; Kolpak, A.M.; Johnston, K.P.; Stevenson, K.J. Water electrolysis on $La_{1-x}Sr_xCoO_{3-\delta}$ perovskite electrocatalysts. *Nat. Commun.* **2016**, *7*, 11053. [CrossRef]
345. Su, J.; Ge, R.; Jiang, K.; Dong, Y.; Hao, F.; Tian, Z.; Chen, G.; Chen, L. Assembling Ultrasmall Copper-Doped Ruthenium Oxide Nanocrystals into Hollow Porous Polyhedra: Highly Robust Electrocatalysts for Oxygen Evolution in Acidic Media. *Adv. Mater.* **2018**, *30*, 1801351. [CrossRef]
346. Lim, J.; Park, D.; Jeon, S.S.; Roh, C.W.; Choi, J.; Yoon, D.; Park, M.; Jung, H.; Lee, H. Ultrathin IrO_2 Nanoneedles for Electrochemical Water Oxidation. *Adv. Funct. Mater.* **2018**, *28*, 1704796. [CrossRef]
347. Sun, X.; Xu, K.; Fleischer, C.; Liu, X.; Grandcolas, M.; Strandbakke, R.; Bjørheim, T.S.; Norby, T.; Chatzitakis, A. Earth-Abundant Electrocatalysts in Proton Exchange Membrane Electrolyzers. *Catalysts* **2018**, *8*, 657. [CrossRef]
348. Liu, B.; Wang, C.; Chen, Y. Surface determination and electrochemical behavior of IrO_2-RuO_2-SiO_2 ternary oxide coatings in oxygen evolution reaction application. *Electrochim. Acta* **2018**, *264*, 350–357. [CrossRef]
349. Cherevko, S. Stability and dissolution of electrocatalysts: Building the bridge between model and "real world" systems. *Curr. Opin. Electrochem.* **2018**, *8*, 118–125. [CrossRef]
350. Chuanpu, H.; Hong, L.; Cangen, M.; Song, Y.; Ma, J. Investigation of Mesoporous Niobium-Doped TiO_2 as an Oxygen Evolution Catalyst Support in an SPE Water Electrolyzer. *ACS Sustain. Chem. Eng.* **2016**, *4*, 746–756.
351. Ju, H.K.; Giddey, S.; Badwal, S.P.S. The role of nanosized SnO_2 in Pt-based electrocatalysts for hydrogen production in methanol assisted water electrolysis. *Electrochim. Acta* **2017**, *229*, 39–47. [CrossRef]
352. Yu, J.-W.; Jung, G.-B.; Su, Y.-J.; Yeh, C.-C.; Kan, M.-Y.; Lee, C.-Y.; Lai, C.-J. Proton exchange membrane water electrolysis system-membrane electrode assembly with additive. *Int. J. Hydrogen Energy* **2019**, *44*, 15721–15726. [CrossRef]
353. Shrinath Dattatray, G.; Prasad Patel, P.; Datta, M.K.; Velikokhatnyi, O.I.; Pavithra Shanthi, M.; Prashant, N.K. First report of vertically aligned (Sn,Ir)O_2:F solid solution nanotubes: Highly efficient and robust oxygen evolution electrocatalysts for proton exchange membrane based water electrolysis. *J. Power Source* **2018**, *392*, 139–149.
354. Wang, Y.; Zhang, L.; Yin, K.; Zhang, J.; Gao, H.; Liu, N.; Peng, Z.; Zhang, Z. Nanoporous Iridium-Based Alloy Nanowires as Highly Efficient Electrocatalysts Toward Acidic Oxygen Evolution Reaction. *ACS Appl. Mater. Interfaces* **2019**, *11*, 39728–39736. [CrossRef]
355. Lu, A.; Peng, D.-L.; Chang, F.; Skeete, Z.; Shan, S.; Sharma, A.; Luo, J.; Zhong, C.J. Composition- and Structure-Tunable Gold–Cobalt Nanoparticles and Electrocatalytic Synergy for Oxygen Evolution Reaction. *ACS Appl. Mater. Interfaces* **2016**, *8*, 20082–20091. [CrossRef]
356. Zhang, B.; Zheng, X.; Voznyy, O.; Comin, R.; Bajdich, M.; García-Melchor, M.; Han, L.; Xu, J.; Liu, M.; Zheng, L. Homogeneously dispersed multimetal oxygen-evolving catalysts. *Science* **2016**, *352*, 333–337. [CrossRef]
357. Xu, L.; Jiang, Q.; Xiao, Z.; Li, X.; Huo, J.; Wang, S.; Dai, L. Plasma-Engraved Co_3O_4 Nanosheets with Oxygen Vacancies and High Surface Area for the Oxygen Evolution Reaction. *Angew. Chem. Int. Ed.* **2016**, *55*, 5277–5281. [CrossRef]
358. Zhou, Q.; Chen, Y.; Zhao, G.; Lin, Y.; Yu, Z.; Xu, X.; Wang, X.; Liu, H.K.; Sun, W.; Dou, S.X. Active-Site-Enriched Iron-Doped Nickel/Cobalt Hydroxide Nanosheets for Enhanced Oxygen Evolution Reaction. *ACS Catal.* **2018**, *8*, 5382–5390. [CrossRef]
359. Anwar, S.; Khan, F.; Zhang, Y.; Djire, A. Recent development in electrocatalysts for hydrogen production through water electrolysis. *Int. J. Hydrogen Energy* **2021**, *46*, 32284–32317. [CrossRef]
360. Wu, Z.P.; Lu, X.F.; Zang, S.Q.; Lou, X.W. Non-Noble-Metal-Based Electrocatalysts toward the Oxygen Evolution Reaction. *Adv. Funct. Mater.* **2020**, *30*, 1910274. [CrossRef]
361. Bidin, N.; Azni, S.R. The effect of magnetic and optic field in water electrolysis. *Int. J. Hydrogen Energy* **2017**, *42*, 16325–16332. [CrossRef]
362. Purnami; Hamidi, N.; Sasongko, M.N.; Widhiyanuriyawan, D.; Wardana, I.N.G. Strengthening external magnetic fields with activated carbon graphene for increasing hydrogen production in water electrolysis. *Int. J. Hydrogen Energy* **2020**, *45*, 19370–19380. [CrossRef]
363. Kaya, M.F.; Demir, N.; Rees, N.V.; El-Kharouf, A. Improving PEM water electrolyser's performance by magnetic field application. *Appl. Energy* **2020**, *264*, 114721. [CrossRef]
364. Costa, C.M.; Merazzo, K.J.; Goncalves, R. Magnetically active lithium-ion batteries towards battery performance improvement. *Iscience* **2021**, *24*, 102691. [CrossRef]
365. Zhang, Y.X.; Fan, L.; Li, X.G. Effect of Alternating Magnetic Field on Electrochemical Behavior of 316L and TA2 in Simulated Seawater. *J. Mater. Eng. Perform.* **2021**, *30*, 9377–9389. [CrossRef]
366. Jing, S.; Hu, H.; Wang, S. Design of pulsed power supply for repetitive pulsed high magnetic field for water electrolysis. *Rev. Sci. Instrum.* **2021**, *92*, 114708. [CrossRef]
367. Li, K.; Zhang, H.; Zheng, X.; Liu, C.; Chen, Q. Hydrogen Production byWater Electrolysis with Low Power and High Efficiency Based on Pre-Magnetic Polarization. *Energies* **2022**, *15*, 1878. [CrossRef]
368. Ren, P.; Pei, P.; Li, Y.; Wu, Z.; Chen, D.; Huang, S. Degradation mechanisms of proton exchange membrane fuel cell under typical automotive operating conditions. *Progr. Energy Comb. Sci.* **2020**, *80*, 100859. [CrossRef]
369. Grigoriev, S.A.; Bessarabov, D.G.; Glukhov, A.S. On the contamination of membrane–electrode assembles of water electrolyzers with solid polymer electrolyte by the elements of titanium alloys. *Russ. J. Electrochem.* **2017**, *53*, 808–817. [CrossRef]

370. Wilberforce, T.; Ijaodola, O.; Ogungbemi, E.; Khatib, F.N.; Leslie, T.; El-Hassan, Z.; Thomposon, J.; Olabi, A.G. Technical evaluation of proton exchange membrane (PEM) fuel cell performance—A review of the effects of bipolar plates coating. *Renew. Sustain. Energy Rev.* **2019**, *113*, 109286. [CrossRef]
371. Stenina, I.A.; Yaroslavtsev, A.B. Low- and intermediate-temperature proton-conducting electrolytes. *Inorg. Mater.* **2017**, *53*, 253–262. [CrossRef]
372. Grigoriev, S.A.; Bessarabov, D.G.; Fateev, V.N. Degradation mechanisms of MEA characteristics during water electrolysis in solid polymer electrolyte cells. *Russ. J. Electrochem.* **2017**, *53*, 318–323. [CrossRef]
373. Apel, P.Y.; Velizarov, S.; Volkov, A.V.; Eliseeva, T.V.; Nikonenko, V.V.; Parshina, A.V.; Pismenskaya, N.D.; Popov, K.I.; Yaroslavtsev, A.B. Fouling and Membrane Degradation in Electromembrane and Baromembrane Processes. *Membr. Membr. Technol.* **2022**, *4*, 69–92. [CrossRef]
374. Zhao, J.; Li, X. A review of polymer electrolyte membrane fuel cell durability for vehicular applications: Degradation modes and experimental techniques. *Energy Convers. Manag.* **2019**, *199*, 112022. [CrossRef]
375. Xing, Y.; Li, H.; Avgouropoulos, G. Research Progress of Proton Exchange Membrane Failure and Mitigation Strategies. *Materials* **2021**, *14*, 2591. [CrossRef]
376. Zatoń, M.; Rozière, J.; Jones, D.J. Current understanding of chemical degradation mechanisms of perfluorosulfonic acid membranes and their mitigation strategies: A review. *Sustain. Energy Fuels* **2017**, *1*, 409. [CrossRef]
377. Yurova, P.A.; Malakhova, V.R.; Gerasimova, E.V.; Stenina, I.A.; Yaroslavtsev, A.B. Nafion/Surface Modified Ceria Hybrid Membranes for Proton Exchange Fuel Cell Application. *Polymers* **2021**, *13*, 2513. [CrossRef]
378. Karpenko-Jereb, L.; Sternig, C.; Fink, C.; Tatschl, R. Membrane degradation model for 3D CFD analysis of fuel cell performance as a function of time. *Int. J. Hydrogen Energy* **2016**, *41*, 13644–13656. [CrossRef]
379. Papakonstantinou, G.; Algara-Siller, G.; Teschner, D.; Vidaković-Koch, T.; Schlögl, R.; Sundmacher, K. Degradation study of a proton exchange membrane water electrolyzer under dynamic operation conditions. *Appl. Energy* **2020**, *280*, 115911. [CrossRef]
380. Li, D.; Motz, A.R.; Bae, C.; Fujimoto, C.; Yang, G.; Zhang, F.-Y.; Ayers, K.E.; Kim, Y.S. Durability of anion exchange membrane water electrolyzers. *Energy Environ. Sci.* **2021**, *14*, 3393–3419. [CrossRef]
381. Dincer, I.; Acar, C. Review and Evaluation of Hydrogen Production Methods for Better Sustain-ability. *Int. J. Hydrogen Energy* **2015**, *40*, 11094–11111. [CrossRef]
382. Kang, X.; Chaperman, L.; Galeckas, A.; Ammar, S.; Mammeri, F.; Norby, T.; Chatzitakis, A. Water Vapor Photoelectrolysis in a Solid-State Photoelectrochemical Cell with TiO_2 Nanotubes Loaded with CdS and CdSe Nanoparticles. *ACS Appl. Mater. Interfaces* **2021**, *13*, 46875–46885. [CrossRef]
383. Nikolaidis, P.; Poullikkas, A. A Comparative Overview of Hydrogen Production Processes. *Renew. Sustain. Energy Rev.* **2017**, *67*, 597–611. [CrossRef]
384. Akhlaghi, N.; Najafpour-Darzi, G. A Comprehensive Review on Biological Hydrogen Production. *Int. J. Hydrogen Energy* **2020**, *45*, 22492–22512. [CrossRef]
385. Franzitta, V.; Curto, D.; Rao, D.; Viola, A. Hydrogen Production from Sea Wave for Alternative Energy Vehicles for Public Transport in Trapani (Italy). *Energies* **2016**, *9*, 850. [CrossRef]
386. Meda, U.S.; Rakesh, S.S.N.; Raj, M.A.L.A. Bio-hydrogen production in microbial electrolysis cell using waste water from sugar industry. *Int. J. Eng. Sci. Res. Technol.* **2015**, *4*, 452–458.
387. Rousseau, R.; Etcheverry, L.; Roubaud, E.; Basseguy, R.; Delia, M.-L.; Bergel, A. Microbial electrolysis cell (MEC): Strengths, weaknesses and research needs from electrochemical engineering standpoint. *Appl. Energy* **2020**, *257*, 113938. [CrossRef]
388. Kadier, A.; Simayi, Y.; Abdeshahian, P.; Azman, N.F.; Chandrasekhar, K.; SahaidKalil, M. A comprehensive review of microbial electrolysis cells (MEC) reactor designs and configurations for sustainable hydrogen gas production. *Alex. Engin. J.* **2016**, *55*, 427–443. [CrossRef]
389. Abanades, S. Metal Oxides Applied to Thermochemical Water-Splitting for Hydrogen Production Using Concentrated Solar Energy. *ChemEngineering* **2019**, *3*, 63. [CrossRef]
390. He, Y.; Hamann, T.; Wang, D. Thin film photoelectrodes for solar water splitting. *Chem. Soc. Rev.* **2019**, *48*, 2182–2215. [CrossRef]